Volume 27
Number 6
June 2025
Pages 1485–1732

Environmental Science
Processes & Impacts

rsc.li/espi

Themed issue: Indoor Environment

ISSN 2050-7887

ROYAL SOCIETY OF CHEMISTRY

PAPER
Trevor C. VandenBoer *et al.*
Commercial kitchen operations produce a diverse range of gas-phase reactive nitrogen species

Environmental Science Processes & Impacts

PAPER

View Article Online
View Journal | View Issue

Cite this: *Environ. Sci.: Processes Impacts*, 2025, **27**, 1517

Commercial kitchen operations produce a diverse range of gas-phase reactive nitrogen species†

Leigh R. Crilley, ‡[a] Jenna C. Ditto, §[bc] Melodie Lao,[a] Zilin Zhou, ¶[b] Jonathan P. D. Abbatt,[c] Arthur W. H. Chan[bc] and Trevor C. VandenBoer *[a]

Gas-phase reactive nitrogen species (N_r) are important drivers of indoor air quality. Cooking and cleaning are significant direct sources indoors, whose emissions will vary depending on activity and materials used. Commercial kitchens experience regular high volumes of both cooking and cleaning, making them ideal study locations for exploring emission factors from these sources. Here, we present a total N_r (tN_r) budget and contributions of key species NO, NO_2, acidic N_r (primarily HONO) and basic N_r (primarily NH_3) using novel instrumentation in a commercial kitchen over a two-week period. In general, highest tN_r was observed in the morning and driven compositionally by NO, indicative of cooking events in the kitchen. The observed HONO and basic N_r levels were unexpectedly stable throughout the day, despite the dynamic and high air change rate in the kitchen. After summing the measured NO_x, HONO and $N_{r,base}$ fractions, there was on average 5 ppbv of N_r unaccounted for, expected to be dominated by neutral N_r species. Using co-located measurements from a proton transfer reaction mass spectrometer (PTR-MS), we propose the identities for these major N_r species from cooking and cleaning that contributed to $N_{r,base}$ and the neutral fraction of tN_r. When focused specifically on cooking events in the kitchen, a vast array of N-containing species was observed by the PTR-MS. Reproducibly, oxygenated N-containing class ions ($C_{1-12}H_{3-24}O_{1-4}N_{1-3}$), consistent with the known formulae of amides, were observed during meat cooking and may be good cooking tracers. During cleaning, an unexpectedly high level of chloramines was observed, with monochloramine dominating the profile, as emitted directly from HOCl based cleaners or through surface reactions with reduced-N species. For many species within the tN_r budget, including HONO, acetonitrile and basic N_r species, we observed stable levels day and night despite the high air change rate during the day (>27 h^{-1}). The stable levels for these species point to large surface reservoirs which act as a significant indoor source, that will be transported outdoors with ventilation.

Received 20th August 2024
Accepted 23rd October 2024

DOI: 10.1039/d4em00491d

rsc.li/espi

Environmental significance

Cooking and cleaning are significant sources of reactive nitrogen species, which are key drivers of the multiphase chemical processes that can lead to poor indoor air quality. Here we present measurements in a commercial kitchen of the total gaseous budget of nitrogenous molecules and demonstrate that a chemically diverse array of nitrogenous species make up about 10% of the total budget. Both cooking and cleaning were found to emit these complex mixtures, while surface reservoirs have a dominant role in controlling their levels. Our observations show that emissions from both sources may be driving complex multiphase chemistry indoors that extends beyond the criterion pollutants and can impact urban air quality.

1. Introduction

Indoor air pollutants are produced, removed, and transformed by many indoor processes including direct emissions, indoor–outdoor air exchange, multiphase chemistry, and surface deposition.[1] Reactive nitrogen (N_r) species, defined here as all N-containing compounds except N_2 and N_2O,[2] are important drivers of indoor air quality due to their chemical activity. Key N_r species include nitrogen oxides (NO_x = NO + NO_2), nitrous acid (HONO), and ammonia (NH_3), which are all known to have detrimental health effects and can be present indoors at levels

[a]Department of Chemistry, York University, Canada. E-mail: tvandenb@yorku.ca
[b]Department of Chemical Engineering and Applied Chemistry, University of Toronto, Canada
[c]Department of Chemistry, University of Toronto, Canada

† Electronic supplementary information (ESI) available. See DOI: https://doi.org/10.1039/d4em00491d

‡ Current address: Atmospheric Services, WSP Australia, Brisbane.

§ Current address: Department of Energy, Environmental, and Chemical Engineering, Washington University in St. Louis.

¶ Current address: Exposure and Biomonitoring Division, Environmental Health Science and Research Bureau, Health Canada.

which exceed outdoor levels by several orders of magnitude.[1] As people spend up to 90% of their time indoors, encompassing time at home and work, a better understanding of the sources and processes driving poor indoor air quality across a diverse range of environments is required.

Cooking and cleaning are known to be significant direct sources of N_r indoors, whose emissions vary depending on the activity type and materials used. Cooking with gas appliances can result in very high direct emissions of NO_x and HONO (mixing ratios up to 400 and 100 parts per billion (ppbv), respectively).[3–8] These sources are especially pertinent in homes that have low ventilation rates or are without a range hood. Under these non-ideal conditions, in a few minutes of use, a natural gas stove can increase NO_2 levels to exceed the 1 h Canadian maximum residential exposure limit (90 ppbv).[9] Transportation of NO_2 indoors is also possible if outdoor levels are high.

The dominant loss of NO_2 from indoor environments can vary, depending on the rate of air exchange. When ventilation is sufficiently high it dominates the removal of NO_2 by transport to the outdoors. The next most important loss is reactive uptake of NO_2 onto indoor surfaces through which HONO will readily form. This HONO can then build up in areas with low levels of indoor lighting (in terms of photon flux and/or energy) and away from windows that generate sunlit areas.[10–12] While the mechanism for surface uptake of NO_2 is debated under typical atmospheric NO_x regimes, the reported association between NO_2 and HONO driven by surface chemistry is strong. The best-described heterogeneous mechanism remains NO_2 hydrolysis, which proceeds through the formation of an N_2O_4 intermediate, ultimately forming HONO and nitric acid (HNO_3) (R1).[12]

$$2NO_2 + H_2O \xrightarrow{\text{surface}} HONO + HNO_3 \quad \text{(R1)}$$

The last indoor sink for NO_2 is through reaction with ozone (O_3). Loss of NO_2 has recently been shown for O_3 in domestic settings where experimental additions have been performed,[13–16] and the reaction is capable of forming the ambient nocturnal pollutants NO_3, N_2O_5, and $ClNO_2$. This has been observed without O_3 addition being required in an athletic facility impacted by polluted outdoor air.[17] Outside of these unique situations, it is not yet clear the extent to which this chemical sink for NO_2 prevails indoors, particularly in domestic settings where the O_3 mixing ratio is known to be low.

Through the loss of NO_2, an abundance of HONO is produced, with studies consistently reporting stable indoor mixing ratios on the order of a few ppbv,[4,18,19] when point sources are not also present. This observation has been explained through theoretical models that use a surface reservoir for HONO,[4] drawing off recent evidence for such outdoors.[18,19] More recently, a study by Wang *et al.*[20] performed ventilation experiments that observed HONO levels rapidly decreasing with increased ventilation (*e.g.* opening doors and windows), followed by a return to the original levels when the ventilation was decreased to the initial state. These observations are consistent with reversible equilibrium partitioning of HONO from a surface reservoir into the overlying air (R2). In this work by Wang and co-workers, surface nitrite (NO_2^-) was also found to be present on the surfaces of deployed glass plates, providing clear evidence from the surface to support this proposed partitioning behaviour.

$$HONO_{(g)} \rightleftharpoons HONO_{(surf)} \rightleftharpoons H_{(aq)}^+ + NO_{2(aq)}^- \quad \text{(R2)}$$

As a result, the equilibrium of HONO from a sufficiently large surface reservoir should always obtain steady state levels under any ventilation regime until the reservoir is depleted. The capacity of such reservoirs, which depends on the effective pH of the surface environment (shown for bulk aqueous exchange in (R2)), and the controls on their dynamics remain open questions.[15] In addition to production from NO_2, other indoor sources of HONO are all thought to be direct emissions and include gas stoves, cigarettes or smoking of other materials, and candles.[11,21] Laboratory experiments have suggested other secondary HONO production routes, such as photo-enhanced reduction of NO_2 on window films containing PAHs,[22] but remain unconstrained for their importance across indoor environments more generally from field observations. Indoor losses of HONO include ventilation, photolysis (R3), and deposition/uptake to surfaces (R2). In all cases, these losses are of concern because of the potential release of the hydroxyl radical (OH) from HONO photolysis, where OH could initiate oxidation chemistry in the presence of organic molecules to form secondary pollutants like O_3 and respirable fine airborne particles ($PM_{2.5}$) indoors and outdoors.[19,23–25]

$$HONO + h\nu \xrightarrow{\lambda < 405\ \text{nm}} NO + OH \quad \text{(R3)}$$

In addition to combustion products, cooking of protein rich food is an important source of N-containing gases and particles indoors, thought to be primarily formed *via* the reaction of amino acids and cooking oils.[26,27] The specific nitrogenous species emitted will vary depending on the fuel, cooking oil, food/ingredients, style (*e.g.*, frying, grilling, baking, *etc.*), temperature, and ventilation.[28] As such, the literature reports a diverse range of gas- and particle-phase nitrogenous species emitted during cooking, and includes NH_3,[29] amides,[28] pyrazine and pyridine derivatives,[30] nitrophenol and nitrobenzenes,[31] heterocyclic nitrogen species, and isocyanic acid (HNCO).[32,33] Overall, cooking is a source of a diverse range of N_r species, where the concentrations of individual compounds are typically low[28,32] and with unknown exposure impact, with the exception of small highly reduced or oxidised N_r species (*e.g.* NH_3, NO).

Cleaning is another primary source of N_r indoors. Elevated levels of chloramines (NH_2Cl, $NHCl_2$ and NCl_3) have been observed indoors after use of chlorinated products, such as bleach-based cleaners that contain HOCl.[17,34–37] The levels of chloramines produced during cleaning can be high, with estimated upper limits of 60, 0.5, and 6.8 ppbv for NH_2Cl, $NHCl_2$ and NCl_3, respectively,[34] which is concerning due to their well-established toxicity. Cleaning is also a source of reduced N_r species, particularly when using ammonium hydroxide-based cleaning products. Ampollini *et al.*[29] demonstrated that using

an ammonium hydroxide cleaner before vinegar (or dilute acetic acid)-based solution resulted in very high NH_3 emissions (>1 ppmv), likely due to acid–base neutralisation on the surface. These studies highlight that surface reactions between cleaning products and/or other sorbed compounds can lead to the release of toxic compounds like NH_3 and chloramines. In addition, other N_r species such as amines or HNCO that are not traditionally measured may be important chemical actors for indoor transformations.[32] Therefore, a budget of total reactive nitrogen is important to ascertain the key species contributing to this chemical pool of species indoors, but one has yet to be established.

Regular high volumes of cooking and cleaning are typical in commercial kitchens (*e.g.* restaurants, catering, *etc.*) and as such are excellent study locations to characterize emissions from these two sources and their interactions,[38] as the rate of these activities is much higher than in residences, which have already been identified for potential impacts on urban air quality.[39] Commercial kitchens are chemically complex spaces influenced by high ventilation rates and are potentially significant sources of indoor and outdoor air pollutants, and yet they are understudied, especially in relation to N_r species. In our companion paper,[40] we explored the indoor exposure and outdoor air transport of cooking and cleaning-derived particulate matter, as well as the unexpected presence of cleaning-derived chlorinated reaction products. The current work presents a time-resolved total gas-phase reactive nitrogen (tN_r) budget in a commercial kitchen, along with contributions from the key species NO_x, HONO and basic N_r (*e.g.* NH_3 and amines) to determine the extent that the budget can be closed. Using supporting measurements from a co-located Vocus proton transfer reaction mass spectrometer (PTR-MS), we seek to identify key N_r species from cooking and cleaning that contribute to the behaviour of the basic fraction of tN_r, as well as the contributors to tN_r that have not been previously speciated; we consider this as a 'missing' fraction in the collective knowledge of the indoor chemistry community. Finally, the role of surfaces as reservoirs that control N_r species capable of partitioning, such as HONO, NH_3, acetonitrile, triethylamine, and monochloramine among many other organic nitrogen-bearing species, will be examined in this space which has long operated as a commercial kitchen where very large surface reservoirs have developed over time.

2. Method

2.1 KOCENA campaign

Full details of the Kitchen Organic Carbon, Emissions, Nitrogen, and Aerosol (KOCENA) campaign will be presented in an overview paper reporting a wider range of observations. Briefly, this study was performed in a commercial kitchen on a university campus in Toronto, Canada from Sept 1–17, 2021. The space is located partially below ground, without any exterior windows to allow sunlight to penetrate in to it. Instead, it is constantly illuminated by light emitting diode fixtures (LEDs). During this sampling period, the kitchen activities ramped up from being closed during lockdown to preparing meals to support on average 300 transactions per day by mid-September, alongside catered orders which could span a few to tens of meals. The kitchen consisted of a large commercial cooking space (henceforth called "main kitchen"), where meals were prepared from the raw ingredients, and a customer-facing food sales area, where meals were ordered, heated, and served. Operating hours were between 8:00–22:00 local time, during which both cooking and cleaning occurred according to health and safety guidelines. Cooking in the main kitchen typically began around 8:00 and concluded around 17:00 between Monday and Friday, while the customer-facing area operated daily. The bulk of cleaning began around 17:00 and continued until closing at 22:00, but was an ongoing periodic activity throughout the day as required by health and safety guidelines. Food sales in the customer-facing area also continued until closing at 22:00. Cooking times for meals or dishes prepared, or cleaning conducted, in the main kitchen were recorded daily by kitchen staff.

2.2 Instrumentation

All instruments were housed in a climate-controlled room and sampled from a common inlet that was located near the highest density of cooking appliances in the main kitchen. The common inlet was 1/4 inch O.D. (0.64 cm) perfluoroalkoxy alkane (PFA) tubing that was 6.6 m long and had a combined total flow of 2.1 litres per minute. The tip of the inlet was positioned to sample from the main cooking area, which included equipment such as ovens, gas stoves, and dishwashers in close proximity – approximately one to three metres away. A polytetrafluoroethylene (PTFE) filter was installed at the entrance of the inlet to prevent intrusion of particles.

2.2.1 tNr instrument description. This instrument, its calibration, and quality control checks have been described in detail by Crilley *et al.*[41] Briefly, it measures the gas-phase tN_r budget and the fractional contribution of key compound classes. The instrument has one sample inlet, which is then directed into one of two pathways, for NO_x or tN_r measurement, in a programmed sequential manner. The NO_x pathway measures NO_x or acidic species within tN_r (N_{r_acid}) *via* selective scrubbing with a sodium carbonate (Na_2CO_3) coated annular denuder, which is introduced to the gas flow using an actuated solenoid valve. The N_{r_acid} fraction is comprised almost entirely of HONO, the dominant gas-phase N_{r_acid} indoors[41] and we therefore refer to this measured fraction as HONO henceforth.

For the tN_r pathway, air is directed to a custom-built Pt catalytic oven held at 800 °C to convert all N_r species to NO_x and it is referred to as the tN_r oven from here onward. Basic species within the tN_r pathway (*e.g.*, NH_3 and amines) are similarly determined by selective scrubbing of the sample gas flow with a phosphorous acid (H_3PO_3) coated annular denuder prior to the sample flow entering the tN_r oven, which will be referred to collectively as $N_{r,base}$. In all cases, NO_x is the measured analyte – as the final combustion product(s) – determined using a commercially available Mo-catalyst chemiluminescent analyser (Serinus 40, American Ecotech LLC, Warren, RI, USA). Automated flow control of the 3-way solenoid valves was

achieved with a LabJack microcontroller and custom LabView program. Calibration, QA/QC, and maintenance activities are provided in Section S1.1 of the ESI.

2.2.2 Vocus proton transfer reaction-mass spectrometry. A Vocus 2R proton transfer reaction time of flight mass spectrometer (Aerodyne Research Inc., henceforth referred to as PTR-MS) was used to measure the chemical composition of volatile organic compounds (VOCs) in the gas phase during KOCENA. Full details can be found in Ditto *et al.*[40] Briefly, the PTR-MS sampled from the common inlet. The PTR-MS inlet flow rate was 110 standard cubic centimetres per minute (sccm) throughout the campaign, and the water vapor reagent flow was maintained at 20 sccm. The ion source was operated at 2.2 mbar in the focusing ion molecule reactor, with a reactor temperature of 100 °C, and a discharge voltage of 430 V. The reduced electric field was estimated to be 130 Td. The mass resolution of the instrument was ~9000 at m/z 200. Only chemicals that were directly calibrated for were converted from ion signal to mixing ratio. Species without a direct calibration are discussed in terms of their ion signal here; we did not apply approaches to estimate their sensitivity in a non-targeted manner due to uncertainty in their chemical structure. Throughout this manuscript, we describe observations of strong ion signals and attribute possible compound identifications where possible. However, we acknowledge that multiple chemical structures may contribute to the signal at any particular m/z (*i.e.*, isomers and fragments of higher molecular weight species). Identifications are provided as examples of contributing species. Details of inlet considerations on transfer delay, calibrations, and data processing are provided in Section S1.2 of the ESI.†

2.2.3 Other supporting measurements. Supporting instruments included an American Ecotech chemiluminescent NO_x (Mo-catalyst, EC9841), and UV-absorption O_3 analyzers (Serinus 10), passive samplers for gas-phase NH_3 and amines. Two measurements of CO_2 and air change rate (ACR) were made: one in the kitchen and the other from the exhaust duct in a mechanical room housing the dedicated exhaust system for the commercial kitchen. Additional details are provided in Section S1.3 of the ESI.†

2.3 Data analysis

All data analysis was performed in R (3.6.3) using R studio. Diurnal trends were calculated using the openair package.[42] As the PTR-MS measured at higher time resolution compared to the tN_r instrument, when calculating diurnal averages, we only included PTR-MS measurements if there was a corresponding tN_r measurement at 1 minute resolution to avoid biasing the mean diurnal trends for comparison. Furthermore, there needed to be at least 25% of tN_r data coverage within any given one-hour period for it to be included in the calculated mean diurnal trends.

2.3.1 Kitchen air change rate calculation. The maximum rotation rate of the exhaust fan of 1750 rpm is equivalent to 25 000 cubic feet per minute (CFM) of ventilation flow. The geometric main kitchen volume was determined to be 617 m^3 by measurement of the dimensions of the walls around the perimeter and throughout the room. These three values were then used to calculate the kitchen air change rate (eqn (1); ACR, h^{-1}).

$$\mathrm{ACR}\ \left(\mathrm{h}^{-1}\right) = \frac{x\mathrm{RPM}}{1750\mathrm{RPM}} \times \frac{25\,000\mathrm{CFM}}{\text{total room volume } \mathrm{m}^3} \times \frac{60\ \mathrm{min}}{h} \times \frac{m^3}{35.31\ \mathrm{ft}^3} \quad (1)$$

2.3.2 Estimating the production rate of HONO from NO_2. A simple box model was constructed to explore the role of HONO surface reservoirs in the commercial kitchen, including the heterogeneous uptake of NO_2 as a source, and photolysis and ventilation as sinks.[4,43] The model terms were constrained by the relevant observations and used to infer surface fluxes.[19,44–46] The details of each term in the model are provided in detail in Section S1.4 of the ESI.

3. Results and discussion

3.1 Measured tN_r budget in a commercial kitchen

The time series of the tN_r and its components (NO_x, HONO and $N_{r,base}$) shows episodic peaks throughout the campaign. In general, spikes in tN_r were observed in the morning and were driven by NO and NO_2, indicating likely cooking events with gas appliances in the kitchen. The short duration of these peaks results from the kitchen ventilation system rapidly removing the emissions.[40] Outside of these peaks, the measured tN_r levels were generally constant over time (Fig. 1). The mean diurnal trends in tN_r also indicate that levels peaked during the morning (6–10 am) and were relatively stable outside of these times (Fig. 2). Overall, the largest single contributor to the tN_r budget was NO_2 (Fig. 2C), followed by $N_{r,base}$ species, NO, then HONO. While the instrument measures the acidic fraction of indoor air ($N_{r,acid}$), this is present dominantly as HONO since prior reports on HNO_3 in indoor air have found very low levels.[47,48]

The average contributions of measured tN_r fractions were fairly consistent between day and night, in the absence of cooking (10 pm to 6 am, Fig. 2B) and when cooking occurred (9 am to 8 pm; Fig. 2C). The clear exception was NO, which accounted for a larger fraction of the tN_r during the day (11%, Fig. 2C), consistent with emissions from gas stove combustion during cooking.[9,49] The observed increase in NO around the typical start of staff-logged cooking activities (6–7 am) was driven in part by intrusion of polluted outdoor air during the start-up period for the ventilation system (Fig. S2†). The HONO and $N_{r,base}$ levels were unexpectedly stable throughout the day (Fig. 2), despite the dynamic and high ACR in the kitchen. This is not driven by inlet effects, as the inlet was shared by the PTR-MS which observed rapid increases and decreases of many polar and oxygenated species related to both cooking and cleaning, and others that demonstrated similar stability.[40] These HONO and $N_{r,base}$ observations point to a significant surface reservoir that has rapid air-surface partitioning[20] and we explore this in more detail below (Sections 3.3.1 and 3.3.5). After summing the

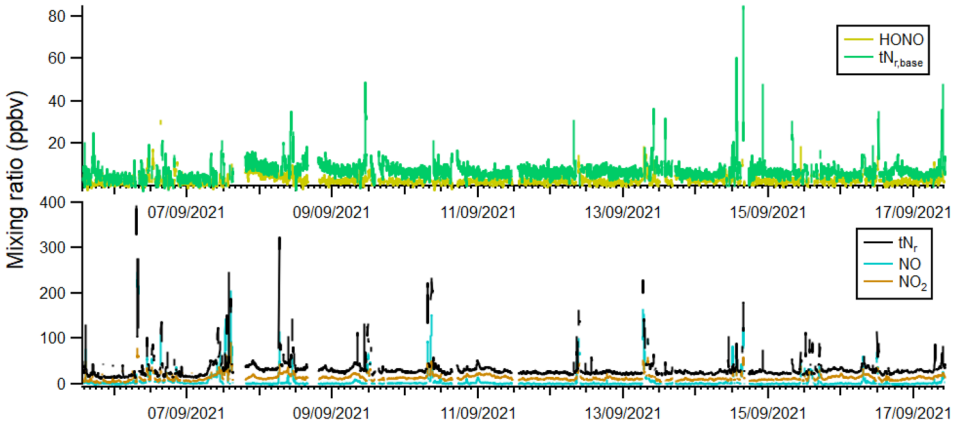

Fig. 1 Time series of (top) the fractions of HONO (yellow) and $tN_{r,base}$ (green) and (bottom) measured mixing ratios of tNr (black), NO (blue), and NO_2 (orange) at a 1 minute time resolution over the whole campaign. Large tick marks denote midnight of each observation day and small ticks mark noon.

measured NO_x, HONO and $N_{r,base}$ fractions, there was on average 5 ppbv of N_r unaccounted for (Fig. 2). This missing fraction of N_r (grey shading in Fig. 2) is expected to be dominated by neutral N_r species based on the sampling strategy of the instrument and is explored further *via* the PTR-MS data in the sections that follow.

3.1.2 Contributions to the basic N_r ($N_{r,base}$) fraction. Ammonia and amines are quantitively converted to NO_x in the tN_r oven.[41] They have been previously shown to be emitted during cooking,[29] and therefore ammonia (NH_3) is expected to be the major component of the $N_{r,base}$ fraction. Due to the more limited nature of indoor amine measurements, we explore this in more detail and refer to this fraction as $N_{r,\ base}$ from here on. Co-located measurements of NH_3 by citric-acid coated passive samplers typically agreed within uncertainty with the mean $N_{r,base}$ levels during the same period (5.7 ± 0.3 and 6.5 ± 3.5 ppbv for passive sampler and tN_r instrument, respectively[41]), consistent with the perspective that NH_3 comprised the majority of the $N_{r,base}$. The dominance of NH_3 is perhaps not surprising as there are many sources in a kitchen, such as cooking of meats as well as cleaning solutions and their reaction products on surfaces.[29] From Fig. 3, the $N_{r,base}$ level was nearly constant at night (5.8 ± 0.4 ppbv) and increased with the start of cooking in the morning, consistent with a source(s) related to kitchen activities that would include cooking and cleaning and/or an increase in temperature driving an increase in the extent of thermodynamic equilibrium partitioning from the surfaces. Increases in temperature of 3 to 6 °C from a consistent nighttime temperature of 26 °C were observed throughout the campaign. The resulting stable $N_{r,base}$ levels of

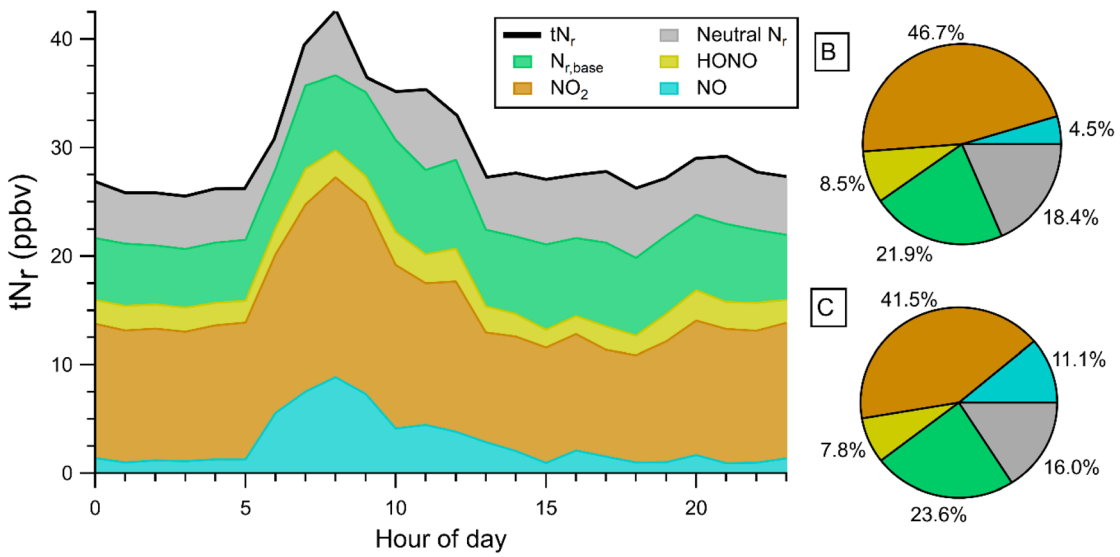

Fig. 2 (A) Mean cumulative diurnal trends of measured tN_r and key species quantified by the tN_r instrument over the whole campaign. Pie charts present the average gaseous N_r budget (B) when operations and occupancy ceased at night (10 pm to 6 am) and (C) during daytime occupancy when cooking was active (9 am to 8 pm).

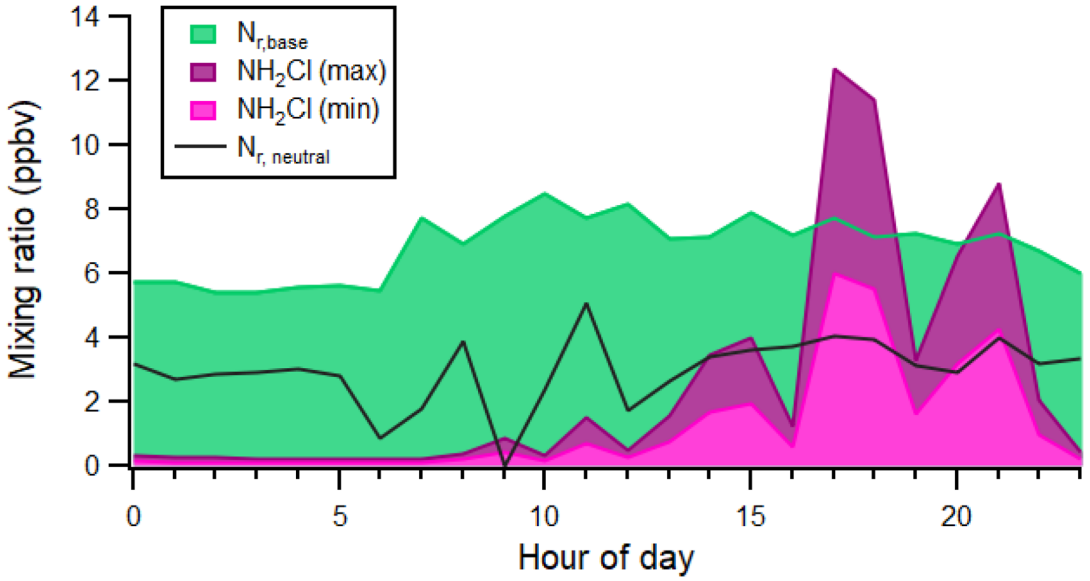

Fig. 3 Mean diurnal trends of measured $N_{r,base}$ and $N_{r,neutral}$ measured by tN_r instrument along with NH_2Cl measured by the PTR-MS. The range of PTR-MS sensitives provides an estimate of upper and lower limits for NH_2Cl mixing ratios as outlined in Ditto *et al.*[40]

6–8 ppbv (Fig. 3), despite the high ACR and this modest temperature increase during the day, also points to a significant surface reservoir for this fraction of the tN_r budget and suggests it is not particularly sensitive to temperature changes under these conditions (see Section 3.3.5).

A vast number of N-containing ions was detected by PTR-MS (see Section 3.2) but here we focus on the basic N_r species class of amines for which the PTR-MS was calibrated using standards of known concentration, namely triethylamine (TEA) and monochloramine (NH_2Cl). Amides, while having known cooking sources,[28] are not expected to be captured by the H_3PO_3 denuder as they are typically very weak bases or even very weak acids. As a strong base that is also volatile, TEA has previously been found to be emitted during fish cooking,[50,51] some instances of which occurred during the measurement period for this campaign. The ambient levels were below the co-deployed passive sampler detection limits for TEA (LOD = 2.59 ppbv for 5 days of collection[52]), while the PTR-MS detected it at levels above its detection limits (on average 25 pptv), with a more detailed discussion on these differences in Section S1.5.†

A major nitrogen-containing compound detected by PTR-MS was monochloramine, NH_2Cl, primarily observed in the afternoon at ppbv levels and in the low pptv range outside of these times (Fig. 3). In the companion paper to this work, cleaning was demonstrated to be the likely source of NH_2Cl at this time[40] consistent with previous reports.[34] Calibration of PTR-MS for NH_2Cl has proven problematic[17,34,36] and in the current work we present sensitivities for NH_2Cl using different approaches, as outlined in Ditto *et al.*[40] Briefly, the sensitivity was determined experimentally,[54] theoretically,[53] and also constrained to measured $N_{r,base}$ levels, in order give a range of possible values (Fig. 3). The three approaches agreed to within a factor of 2, thus the true NH_2Cl mixing ratio likely lies within this range. However, this also suggests that NH_2Cl would have accounted for a significant fraction of the $N_{r,base}$ (42–88%) during the afternoon when levels peaked despite our knowledge that the NH_3 levels agreed well through the independent verification by passive samplers, but which do not provide time-resolved insight.

Our calculation assumes that NH_2Cl was quantitively converted to NO_x in the tN_r oven and/or scrubbed with the H_3PO_3 denuder. These have not been experimentally determined to be true due to the difficulty in generating stable gas-phase levels of NH_2Cl.[34,55] This assumption may not be valid, at least for complete (*i.e.* 100%) conversion or scrubbing of NH_2Cl, as we did not observe a notable increase in $N_{r,base}$ during the afternoon when NH_2Cl levels peaked for extended periods of time (Fig. 3). While the estimated range of NH_2Cl levels were generally within the total amount of measured $N_{r,base}$ (Fig. 3), it seems unlikely that NH_2Cl would account for the vast majority $N_{r,base}$ in the afternoon. For this to be true, the levels of other $N_{r,base}$ species (*e.g.* NH_3) would have had to correspondingly decrease, which is unlikely as NH_3 is emitted during cleaning,[29] and cooking was still occurring at this time. Fig. S3† demonstrates that when there was a peak in NH_2Cl (up to 80 ppbv, 9:25–9:45 pm), the measured tN_r, and the $N_{r,neutral}$ fraction in particular (Fig. 2), did increase relative to previous or later measurements when NH_2Cl was notably lower. The magnitude of the missing fraction in $N_{r,neutral}$ (Fig. 3, black line) would suggest that the tN_r instrument is responding to NH_2Cl because it is passing through the H_3PO_3 denuder either entirely or in part. This is possible, as these molecules are less polarizable and weaker bases than NH_3. Similarly, NH_2Cl is less likely to adsorb or ionize on surfaces conditioned with atmospheric water vapour and be less subject to inlet effects compared to NH_3, which transfers readily from our instrument characterization.[41] The conversion efficiency of NH_2Cl in the catalytic oven should be substantial, based on the oven being

characterized to do this to alkylamines, but whether the conversion is quantitative is not currently known. Comparing the magnitude of our estimated mixing ratios of NH_2Cl to the PTR-MS theoretical calibration factor, a lower limit, there is good agreement (3–4 ppbv) and some consistent features in the time trends. At the experimental calibration factor limit, however, a substantial disagreement emerges (4–8 ppbv difference). The observed high levels of NH_2Cl in this study were a surprise and future work will seek to improve the tN_r instrument performance with respect to chloramines, as these are increasingly being recognized as compounds of interest in both indoor and outdoor environments.[17,34,36,54] These improvements would likely be by increasing the combustion temperature to 825 °C or greater, in line with our related work on total chlorine detection.[56]

3.1.3 Contribution of neutral species to the tN_r budget. A notable fraction of the commercial kitchen tN_r budget was not accounted for by NO_x, HONO or $N_{r,base}$ during both in-use and idle periods (*ca.* 16%, 5 ppbv; Fig. 2). The co-located PTR-MS was calibrated for a number of N containing ions that would not have been part of either the acidic or basic fractions of the tN_r and included $C_2H_3N^+$ (calibrated with acetonitrile), $C_3H_7NO^+$ (calibrated with propionamide), $C_4H_5N^+$ (calibrated with pyrrole), $C_3H_3N^+$ (calibrated with acrylonitrile).[28] Acetonitrile has multiple indoor sources including cooking, combustion, and tobacco smoke, where the latter is banned from public indoor spaces in Canada.[32,40,57,58] Propionamide, pyrrole and acrylonitrile are known to be emitted by cooking,[32,59] and pyrrole has been identified in a suite of volatile molecules measured in coffee aroma.[60] The quantities of these neutral N-containing species were therefore included in our mass balance to see the extent to which they close the tN_r budget (Fig. 4). Acetonitrile accounted for roughly a quarter of the missing neutral fraction of tN_r, with mean levels of 1.1 ppbv, representing 4% of the overall mean tN_r. This was followed by propionamide (mean of 0.72 ppbv, 2.5% of the tN_r). The other two calibrated N-species, pyrrole and acrylonitrile combined for <0.5% of mean tN_r. The higher contributions from acetonitrile likely reflect the intense cooking in this space,[40] with higher levels observed here during the day when cooking was occurring in the kitchen (Fig. S4†). The observed levels of acetonitrile may also reflect contributions from other sources, such as third hand tobacco smoke or a surface reservoir and is explored in more detail below (Section 3.3).

It is important to note that the levels reported in the previous paragraph are mean diurnal levels over the whole campaign, and the contributions from N-containing species during cooking events may be higher,[40] which is explored in detail in the next section. Overall, with the addition of these four neutral N-containing species, roughly 3 ppbv of the tN_r was still unaccounted for by mass balance, with the variability in mean tN_r levels on the order of ±4 ppbv. Therefore, much of the missing fraction could reside within the tN_r instrument uncertainty (20%, (ref. 41)), yet 3 ppbv is also not a negligible amount. We suggest that this points to contributions from other N-containing species that were detected, but that the PTR-MS was not directly calibrated for. One such species could be isocyanic acid (HNCO), shown in recent work to be present in the ppbv range after cooking and cleaning activities in a house.[32]

3.2 Cooking and cleaning as a source of multiple gas-phase N-containing species

3.2.1 Observed cooking plumes in the kitchen. The tN_r instrument time resolution prevents it from detecting peaks related to cooking emission that are rapidly ventilated, or at a minimum, they were not captured fully. Cooking analyte peaks, like NO measured by the second supporting analyzer,

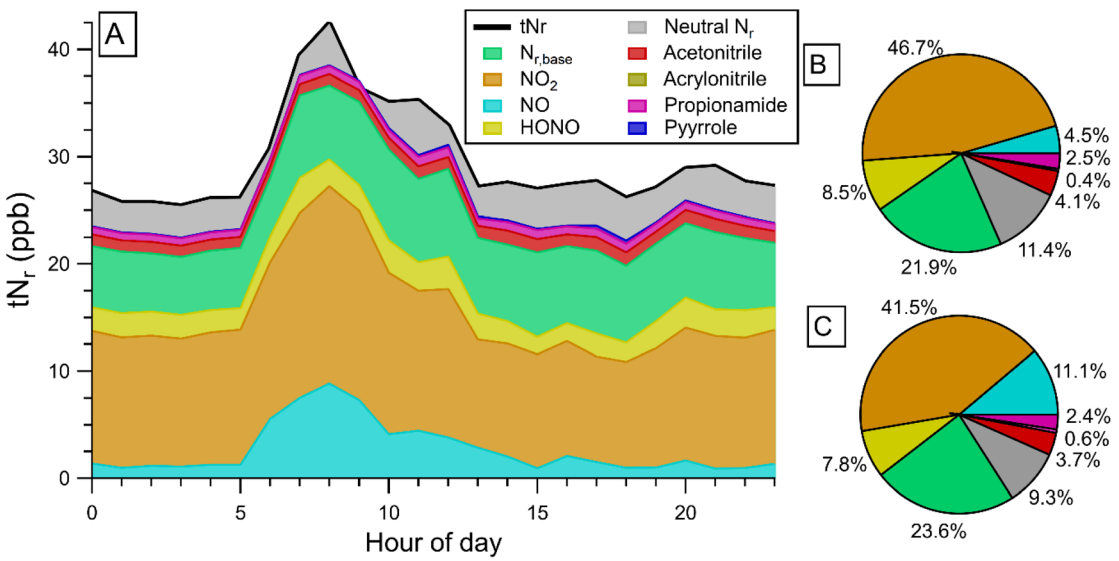

Fig. 4 (A) Cumulative mean diurnal trends of quantified tN_r and sub-species along with calibrated N-containing ions thought to arise from neutral molecules detected by PTR-MS. Pie charts represent the average gaseous N_r budget (B) at night when operations ceased (10 pm to 6 am), and (C) during occupation for daytime cooking (9 am to 8 pm).

were observed to typically last for a shorter time than our 20 minute duty cycle. In this section, we focus on the PTR-MS dataset to explore cooking emissions of N-containing ions, and therefore are excluding NO_x, HONO and NH_3 emissions. In this section, an adapted plume analysis was used to explore the chemical composition of cooking related emissions, outlined in detail previously.[40] Briefly, a cooking plume/event was identified when at least three of the five selected cooking tracers increased simultaneously above background levels: acrolein, methanol, sum of BTEX (benzene, toluene, ethylbenzene and xylenes), CO_2, and/or NO. This approach quantified cooking emissions above the observed backgrounds and gives insight to the complexity of emissions resulting from the high levels of activity/cooking in the kitchen. The full approach is discussed in detail in Ditto *et al.*[40]

3.2.2 Nitrogen containing ion classes observed during cooking. The relative contributions of each class of nitrogen-containing compounds varied across different events. During the chemically identified cooking events, the main class of nitrogen-containing ions detected across all the events was $C_{2-10}H_{3-23}N_{1-3}$ (31%, Fig. 5). Apart from this, there appeared to be two broad groups, where some events were dominated by $C_{1-5}H_{2-10}N_{0-1}Cl_{1-2}$ ions, while others were characterized by higher levels of $C_{2-10}H_{3-23}N_{1-3}$ and/or $C_{1-12}H_{3-24}O_{1-4}N_{1-3}$ ions. From Fig. 5, events that were characterized by higher levels of $C_{2-10}H_{3-23}N_{1-3}$ and/or $C_{1-12}H_{3-24}O_{1-4}N_{1-3}$ class ions were generally observed during the typical cooking periods for the main kitchen (8 am to 3 pm), as might be expected. The largest class of N-containing ions was amines or other reduced nitrogen species ($C_{2-10}H_{3-23}N_{1-3}$) and all the cooking events identified in Fig. 5 had notable contributions from ions in this class. Overall, 35% of detected ions with an assigned molecular formula were N-containing (108 out of 308 in total) with the rest containing other combinations of carbon, hydrogen, and oxygen atoms, with smaller contributions from sulfur, chlorine, and silicon. Many of the major ions in the $C_{2-10}H_{3-23}N_{1-3}$ and $C_{1-12}H_{3-24}O_{1-4}N_{1-3}$ classes are likely unsaturated or cyclic compounds. For reduced nitrogen species, some of the top ions detected included the calibrated neutral N_r species identified earlier; acetonitrile, pyrrole and acrylonitrile ($C_2H_3NH^+$, $C_4H_5NH^+$ and $C_3H_3NH^+$, respectively), which have known cooking sources[61] and combustion sources[62] and are unsaturated compounds. We note that the ion signals shown in Fig. 5 are influenced by their ionization efficiency by proton transfer, but we show them here to highlight the diversity of species observed and their overall trends during cooking events.

The time series of these ions revealed episodic peaks and higher levels during the morning to early afternoon (Fig. S4 and S5†), consistent with a period of expected cooking-related emissions in the kitchen and outdoor surveys conducted on

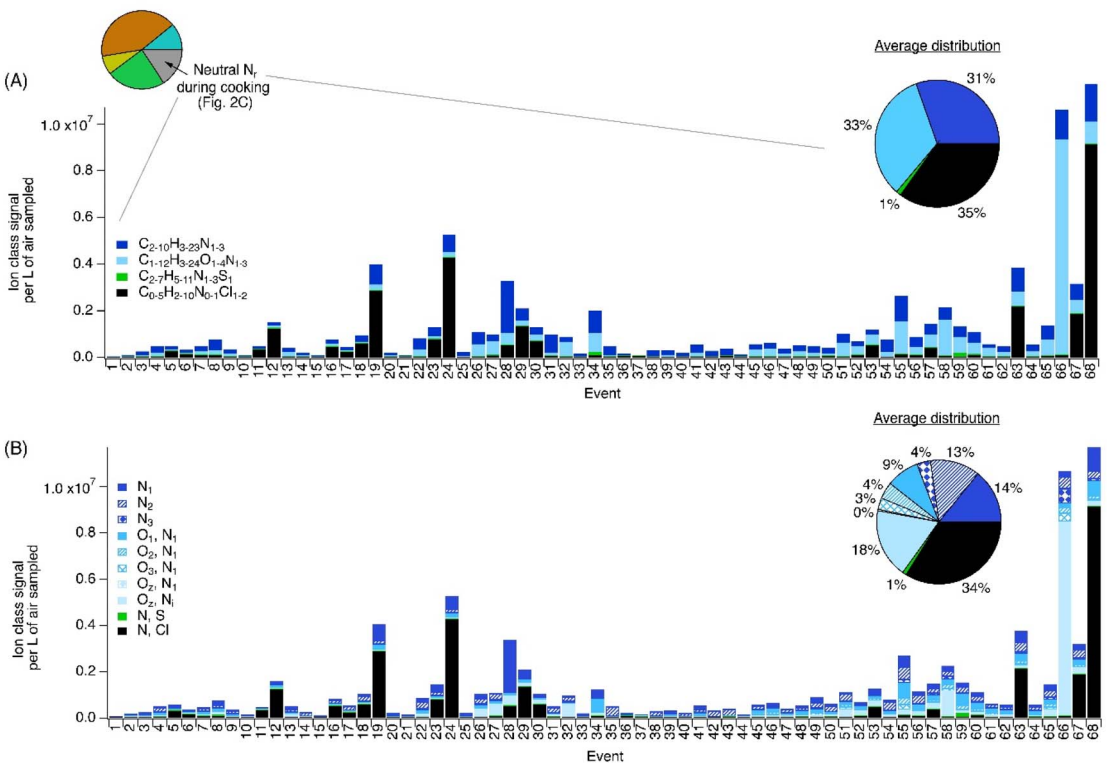

Fig. 5 (A) Nitrogen containing ion signal fractionation for each of 68 distinct cooking events throughout the sampling campaign. (B) Nitrogen specific and associated heteroatom signal groupings. We note that the data shown in (B) is the same as the data shown in (A), but further broken down by the number of N and O atoms to describe the formulas in additional detail. A description of the cooking events is available in Ditto *et al.*[40] The pie charts illustrate the average ion class distribution across all events. In panel B, *i* and *z* subscripts are used to reflect the number of N atoms being >1 and the number of O atoms being >3, respectively. For comparison with the tN_r data, we also included the daytime pie chart from Fig. 2C here, to illustrate the further chemical speciation of neutral N_r segment that we explored here with the PTR-MS during cooking events.

commercial kitchen plumes.[38] Other uncalibrated amine ions consistently detected at high levels with similar temporal and diurnal trends were possible cyclic amines $C_5H_5NH^+$ (suggested to be pyridine, Fig. S6†) and $C_6H_8N_2H^+$ (suggested to be alkylpyrazine, Fig. S7†). Pyridine is known to be emitted during meat roasting,[63] while alkylpyrazine has been associated with the aroma of foods, including coffee[64] and baked potato.[65] The observations of these ions combined with the observed temporal patterns, points to a cooking-related source for $C_5H_5NH^+$ and $C_6H_8N_2H^+$. Cooking was not the only likely source of ions in the $C_{2-10}H_{3-23}N_{1-3}$ class, with the ion $C_5H_9NH^+$ having very similar diurnal trends to NH_2ClH^+ (Fig. S8†) which points to cleaning as another source of this nitrogenous ion (Section 3.2.4).

3.2.3 Meat cooking as a source of nitrogen containing ions. Closer inspection revealed that events dominated by $C_{1-12}H_{3-24}O_{1-4}N_{1-3}$ ions (*e.g.* events 26, 34, 45, 51 and 66) occurred generally during times when meat dishes were logged as being cooked in the main kitchen. Cooking event 66, which had the highest contribution from oxygenated N-containing ions, occurred when tagine, butter chicken and lentil dishes were logged. This event was dominated by the $C_4H_8N_2O_3H^+$ ion, which could be attributed to the amino acid asparagine, which is enriched in meat and legumes, and therefore these may have been the source. A possible fragment of asparagine, with ion formula $C_4H_3NO_2H^+$ (*i.e.*, asparagine after the loss of water and ammonia) was also observed with lower signal; this ion was observed prominently in laboratory experiments where pure asparagine was heated in cooking oil and volatile products were measured with this same PTR-MS.[28] In laboratory experiments, signal was dominated by this fragment and asparagine itself volatilized very little, whereas in these field measurements, $C_4H_8N_2O_3H^+$ (possibly asparagine) has significantly greater signal than its fragment. It is unclear whether this fragment was formed due to thermal decomposition of the asparagine precursor,[66] the PTR-MS ionization region, or a combination of both. However, the increased prevalence of the parent ion in field measurements could suggest cooking conditions that allowed for its volatilization more readily without in-field fragmentation, such as reduced cooking temperatures relative to lab experiments.

These dishes were also cooked at other times (*e.g.* events 27, 32 and 58 for butter chicken, tagine and lentils, respectively) and while these events also had high contributions from $C_{1-12}H_{3-24}O_{1-4}N_{1-3}$ ions and specifically $C_4H_8N_2O_3H^+$ (Fig. 5A), the levels were not as high and may be because of the location of preparation or the procedure used (*e.g.* extent of covering, duration, maximum temperature, *etc.*). Other cooking related ions were observed in the $C_{1-7}H_{5-11}N_{1-3}S_1$ ions class, which only accounted for a small fraction (1%, Fig. 5) of nitrogen containing ions detected across all the events. The major ion in this class was possibly a thiozoline ($C_5H_8N_2OSH^+$), previously associated with meat aromas[67] and could originate from a cooking-related source.

As cooking is demonstrated here to be a likely major source of the $C_{2-10}H_{3-23}N_{1-3}$ and $C_{1-12}H_{3-24}O_{1-4}N_{1-3}$ classes of ions, we compared the ions detected during selected cooking events with those emitted during a controlled laboratory study that simulated cooking processes by heating amino acids with triglycerides (cooking oil).[28] During this work, Ditto *et al.*[40] observed that the reactions between thermal degradation products of triglycerides and amino acids (forming NH_3 upon heating) resulted in the emissions of numerous amides. Fig. S10† demonstrates that there was 15% overlap with ions from simulated cooking emissions and a preparation of chicken, salmon, and vegetable in the kitchen cooking logs. A similar comparison showed this overlap rose to 30% for a pork and vegetable cooking event (Fig. S9†). Some of the major N-containing ions that were observed to overlap were $C_2H_3NH^+$ (acetonitrile) and $C_4H_7N_3H^+$ as well as oxygenated N-containing ions such as CH_3NOH^+, suggesting that meat cooking is a source of molecules that are precursors to these ions. The oxygenated N-containing ions observed in both studies, such as CH_3NOH^+ were probably amides, which are known to be toxic.[28] We cannot definitively assign these ions to amides from these field measurements, as structures cannot be unambiguously ascertained by PTR-MS. Interestingly, many N-containing ions in this class designation (85 and 70%, by ion intensity; Fig. S9 and S10†) were not observed to overlap with the simulated meat cooking emissions study,[28] suggesting that cooking related sources of this compound class are highly variable under realistic conditions where many protein sources and combinations of oils may be used simultaneously, similar to the observations reported by Coggon *et al.* in Las Vegas.[68] This highlights the complexity of N_r species emitted by cooking, as the vast majority were not emitted during the controlled lab experiments of meat cooking in heated oil, which could be one major cooking source of amides.[69,70]

The complexity of cooking emissions in the kitchen, due to the mixture of two different cooking areas, combinations of different ingredients, overlapping preparations, and potentially different procedures and appliances being used on any given day, makes it challenging to isolate useful tracer ions for a particular dish or even a single form of food. In general, oxygenated N-containing class ions ($C_{1-12}H_{3-24}O_{1-4}N_{1-3}$), consistent with the known formulae of amides or combinations of reduced nitrogen groups (*e.g.*, amines) with oxygenated groups, appear to be good tracers for meat cooking although identifying all tracer ions was not possible and could be the focus of future targeted research under controlled lab conditions.

3.2.4 Cleaning as source of chloramines. Many of the top N-containing ions measured by the PTR-MS were chlorinated (Fig. 5B), accounting for around 35% of all nitrogen-containing ions during the selected distinct events (Fig. 5A). Closer inspection revealed that events with high proportions of $C_{1-5}H_{2-10}N_{0-1}Cl_{1-2}$ ions (*e.g.* events 11, 12, 19, 24, 29, 63, 67 and 68) typically occurred in the afternoon (after 4 pm) when both cleaning and, to a lesser extent cooking, were occurring in the kitchen. In this ion class, NH_2ClH^+ had the highest signal intensity and was attributed to monochloramine.

The levels of NH_2ClH^+ maximized in the afternoon (Fig. 3) and in our companion paper,[40] where cleaning emissions were determined to be the dominant source of this species.

Specifically, the use of cleaning products containing sodium hypochlorite in the kitchen were likely primary drivers, either through direct emissions[37] or *via* surface reactions with N-containing compounds such as amines (*e.g.* ammonium salts, long chain alkyl amines, monoethanolamine) that were also present on surfaces or in other cleaning solutions. In contrast to previous reports of bleach cleaning in a residential house,[34,37] we did not observe elevated ion counts that could be assigned to $NHCl_2H^+$ or NCl_3H^+ by PTR-MS during cleaning activities in the kitchen.[40] This was likely due to the inability of this PTR to detect these compounds with more chlorine atoms.[54] Regardless, our observed NH_2ClH^+ during cleaning is similar to a recent report from indoor sports centres[36] and may reflect the prevalence of substantial cleaning emissions of this molecule from large-scale/commercial environments compared to domestic settings. Other prominent chlorinated N-bearing ions with greater hydrocarbon character were readily observed and included $C_5H_{10}ClNH^+$, $C_3H_6ClNH^+$, $C_2H_4ClNH^+$ and CH_4ClNH^+, which are thought to originate from unique parent compounds (*i.e.* not as a result of fragmentation in the PTR-MS[40]). The $C_{1-5}H_{4-10}ClNH^+$ ion series were likely *N*-chloraldimines, which are formed from the reaction of HOCl and amino acids on surfaces.[35] Since amino acids are expected to be ubiquitous on kitchen work surfaces from food material transfer as a source, the observed ions for these reaction products would be ever-present due to the stringent cleaning procedures to maintain health and safety in a commercial kitchen work environment.

3.3 Surfaces are significant reservoirs of N_r in the kitchen

3.3.1 Reservoirs and partitioning fluxes of nitrous acid (HONO). Throughout the measurement period, mixing ratios of HONO had stable background levels with an average of 2.4 ± 2.0 (1σ) ppbv, (Fig. S11†) in the absence of direct emissions from cooking (Fig. 1, Section 3.2.1). Average daytime and nighttime levels of HONO were similar at 2.5 ± 2.1 and 2.4 ± 1.3 ppbv, which was surprising since ACR was measured to be 27.2 changes per hour, on average, when the kitchen was in use, and was likely between 1.0 to 0.1 h^{-1} from natural air infiltration processes when operations were ceased and all active building ventilation was off, respectively. These values span a typical range reported for residences and we assume the same applies to most modern building envelopes.[71] We were unable to find reports of infiltration rates for commercial spaces with inactive ventilation. Given that the space had been unused for over a year prior to our measurements, we expected these pollutant levels to be at a minimum at the start of the campaign, increasing as the activities in the kitchen ramped up in duration and intensity over the observation period, similar to HONO accumulation following a Thanksgiving dinner prepared during the HOMEChem campaign.[49] Since this was not the case, the similarity between daytime and nighttime averages therefore points to gas-phase HONO being in equilibrium with a very large reservoir present on the surfaces in the kitchen and throughout any hidden spaces (*e.g.* above drop ceilings, in porous materials, air supply ducts, *etc.*[61]).

A well-recognized precursor to HONO in any environment is NO_2, so the interplay of these two species was explored first. Heterogeneous surface uptake is expected to be an important loss process of indoor NO_2 as these environments have high surface area to volume ratios (S/V), with a lower limit value of 3.2 m^{-1} calculated for this commercial kitchen, ignoring the surfaces provided by appliances, shelving and materials thereon, as well as their porosity.[12,72–74] Outdoors, the conversion of NO_2 to HONO on surfaces has been implied through the ratio of $HONO/NO_2$ relative to NO_x emitted directly from vehicle combustion ($HONO/NO_x = 0.5–2\%$).[75–78] Indoors, in the absence of a direct HONO source, it can be used similarly to infer the potential for this heterogeneous NO_2 chemistry as a source of HONO.[79] Here, the background $HONO/NO_2$ ratio in the absence of direct sources of either molecule in the kitchen was on average 0.19 ± 0.03, with little diurnal variation observed, despite the difference in ACR during operating hours and at night. The consistently high $HONO/NO_2$ therefore points to heterogeneous reactions on surfaces acting as an source of gas phase and reservoir HONO.[20] This ratio is also lower than that reported for direct HONO emissions from gas stoves, which have found ranges of $HONO/NO_2$ spanning 0.5 to 1.0 depending on the duration of gas stove operation, with 1.0 being the most commonly observed.[4,5] Therefore, if cooking emissions were not rapidly ventilated, it might be reasonable to expect that HONO was deposited to surfaces in addition to the heterogeneous reaction of NO_2, prior to the upgraded HVAC being installed in this space a few years prior to this study.

3.3.2 Surface reservoir for NO_2. Like HONO, the NO_2 mixing ratios were unexpectedly constant and elevated in the kitchen throughout the campaign (13 ± 2.3 ppbv, 1σ), as measured by both NO_x analyzers. These were in contrast to the lower mixing ratios with typical diurnal traffic patterns in NO_2 observed outdoors (1–34 ppbv; 6.3 ± 4.7 ppbv, 1σ; Fig. S2†) from a local air quality monitoring station. Outdoor mixing ratios were similar to those indoors on mornings when local highway and direct emissions were present but typically lower by several ppbv compared to the indoor amounts (Fig. S2†). When outdoor pollution was brought indoors, the mixing ratio of NO_2 increased on top of the stable background of 13 ppbv (Fig. S2†). The standalone NO_x analyzer also did not observe NO_2 persisting in the kitchen from point sources such as the gas stoves, as spikes during known cooking times were rapidly ventilated (<7 minutes; Fig. 1 and S1†). In the case of directly emitted NO being transformed, there was insufficient time for substantial NO_2 formation from reaction with O_3 due to this same rapid ventilation during in-use periods of the kitchen. Therefore, this suggests that the kitchen surfaces also act as a reservoir for NO_2, consistent with recent reports from a test house[15] and an in-use residence[5] demonstrating similar findings. In this commercial kitchen, the space experienced lower rates of ventilation in the past so the reservoir may have accumulated substantially in prior years leading to the higher levels observed here compared to the two home studies. With the more recent installation of the current ventilation system, there may be a slow reversal of this process for both HONO and NO_2 but such a trend did not present itself during this 3 week observation period.

3.3.3 Chemical box model of known HONO sources and sinks. To obtain a better understanding of the relative role of surface exchange of HONO, a simple chemical model was constructed with the known processes that influence the temporal behaviour of HONO in the kitchen (eqn (6); Section S1.4). From measured plumes of NO_2 during cooking, alongside the measured ACR values, an upper limit of the reactive uptake coefficient (γ_{NO_2}; eqn (2)) was constrained for the disproportionation reaction that generates HONO. A γ_{NO_2} of $3.8 \pm 2.4 \times 10^{-5}$ was calculated from the observed k_{rem,NO_2} of 26 ± 16 h^{-1} calculated from the six events where NO_2 decay was faster than the measured ACR (Fig. S1†). In former indoor work that constrained surface uptake values using NO_2 decay rates, the full range of potential loss rates was easier to determine because ACR was much lower at 0.5 ± 0.1 h^{-1},[4,5,49] which is a typical rate for homes,[71] and similar to the assumed rate in this commercial kitchen at night when the forced air ventilation was off and operations ceased. Given the highly ventilated conditions during working hours, γ_{NO_2} less than 1.4×10^{-5} would not be possible to observe and would represent the upper limit for the remaining 17 observed NO_2 plumes during cooking. It is therefore instructive to compare this same chemistry against values reported for a range of other surfaces to establish likely boundaries and a best estimate to represent this chemistry in a model framework (Section S2; Table S2†). These include a residential kitchen where γ_{NO_2} was $1–2.3 \times 10^{-6}$, or from lab studies on a wide range of environmentally-relevant substrates where γ_{NO_2} ranges from 1×10^{-6} to 1×10^{-5}.[44,75,80–83]

Competing with the heterogeneous surface source of HONO (Fig. 6, top) are losses by air exchange and photolysis (Fig. 6, middle). The measured spectral irradiance in this space, despite lighting being on 24 hours per day, 7 days per week, was generated from LEDs overhead in place of traditional fluorescent tubes,[84] where the new lighting ($\lambda > 405$ nm) did not provide photons with high enough energy to facilitate meaningful photolytic loss of HONO. As a result, the majority of HONO loss within the kitchen was driven by ventilation to the outdoor environment, which was then rapidly replaced from the surface reservoir on the timescale of our observations (~1–5 min). From this simple box model, the predicted HONO was found to be substantially lower than the measured HONO and generally followed the same trends, but inverted in sign, due to the strong impact of the ventilation on the fate of molecules in this space (Fig. 6, bottom). Additional sources of HONO are required to reconcile the difference between the model and observations and was true for both boundary condition scenarios for this model (Table S2†).

Comparing the measurements to the production of HONO from NO_2 in the model, outdoor to indoor transport could partially reconcile the observations (Section S2.1†), but the discrepancy persists throughout the day regardless of whether the ventilation is active (Fig. 6). As a result, we conclude that outdoor HONO transported indoors was unlikely to have played a substantial part in the overall temporal dynamics or magnitude of HONO in this space, but it may contribute in the morning when the probability was highest. Similarly, due to the low energy LED lighting and absence of windows, we are able to rule out photochemical contributions. Overall, comparing the predicted production rate of HONO and the measured values confirms that, throughout all hours, HONO in the commercial kitchen is overwhelmingly produced by release from a surface reservoir, followed by heterogeneous uptake of NO_2 (Fig. 6). Even when the ACR is high, the indoor HONO concentration remains constant despite being removed in abundance (Fig. S12–S14), such that the high rate of transfer is most likely explained by sustained surface emissions. With all seven days showing the same trends in Fig. 6, it is not surprising to find a dynamic situation from the measured to predicted ratio for HONO chemistry in this space. This is because the cooking activities and ACR were similarly dynamic. The overall diurnal campaign averages provide broader insight into the general drivers of HONO chemistry in this busy indoor space (Fig. 7). From this, we consider the relative roles of NO_2 and surfaces in the two disparate daytime and nighttime ACR regimes in more detail to investigate their dynamics.

3.3.4 Boundary cases for surface chemistry for HONO and NO_2. At night when the HVAC system is off and the kitchen is considered unventilated, the situation is simple, as the predicted HONO from the measured NO_2 uptake was insufficient to explain the observed levels (Fig. 7). This strongly suggests surface emissions dominate HONO production. The predicted HONO levels are never higher in the model compared to the observations, for any scenario (Table S2†), so there are no times when the surface reservoir is being recharged by deposition (Fig. 7). The production of HONO from NO_2 was, on average, 5% of that calculated from surface fluxes to maintain HONO in our best estimate model, and 53% when using the highest conversion rate for NO_2 and lowest ACR_{night} values. During the day, the predicted HONO values become strongly negative, as the ACR losses are capable of completely ventilating the volume of the kitchen more than ten times in a given hour. The difference between predicted and measured HONO concentrations at these times ranges from about 6×10^{10} to 1×10^{11} molecules cm^{-3} (Fig. 7 and S12–S14†) which is equivalent to mixing ratios of 2.5 to 4 ppbv of HONO present in the room air. Therefore, this corresponds to the entirety of the observed mean HONO levels which implies that the surface source is always the most important HONO production mechanism, exceeding NO_2 hydrolysis by a factor of 50 or more during the operating hours of this commercial kitchen (Fig. 7). Recall that we also observed the impact of direct cooking emissions to be short-lived under the modern HVAC operations in this space (see above).

A mean surface emission flux of 7.4×10^8 molecules cm^{-2} s^{-1} exists during the high ACR operating hours (8 am to 10 pm). In comparison both Wang *et al.*[49] and Collins *et al.*[4] observed fluxes in the range of 2.2 to 2.9×10^7 molecules cm^{-2} s^{-1} for ACRs from 0.0 to 1.0 h^{-1} during rapid ventilation experiments, where time constants to recover from the perturbation were used to determine HONO fluxes. Our fluxes, to maintain similar indoor HONO mixing ratios, are 20 times larger or more, consistent with the potentially higher surface loadings, S/V and/or porosity of the kitchen materials in which a reservoir has been built up historically with low ventilation, and/or the

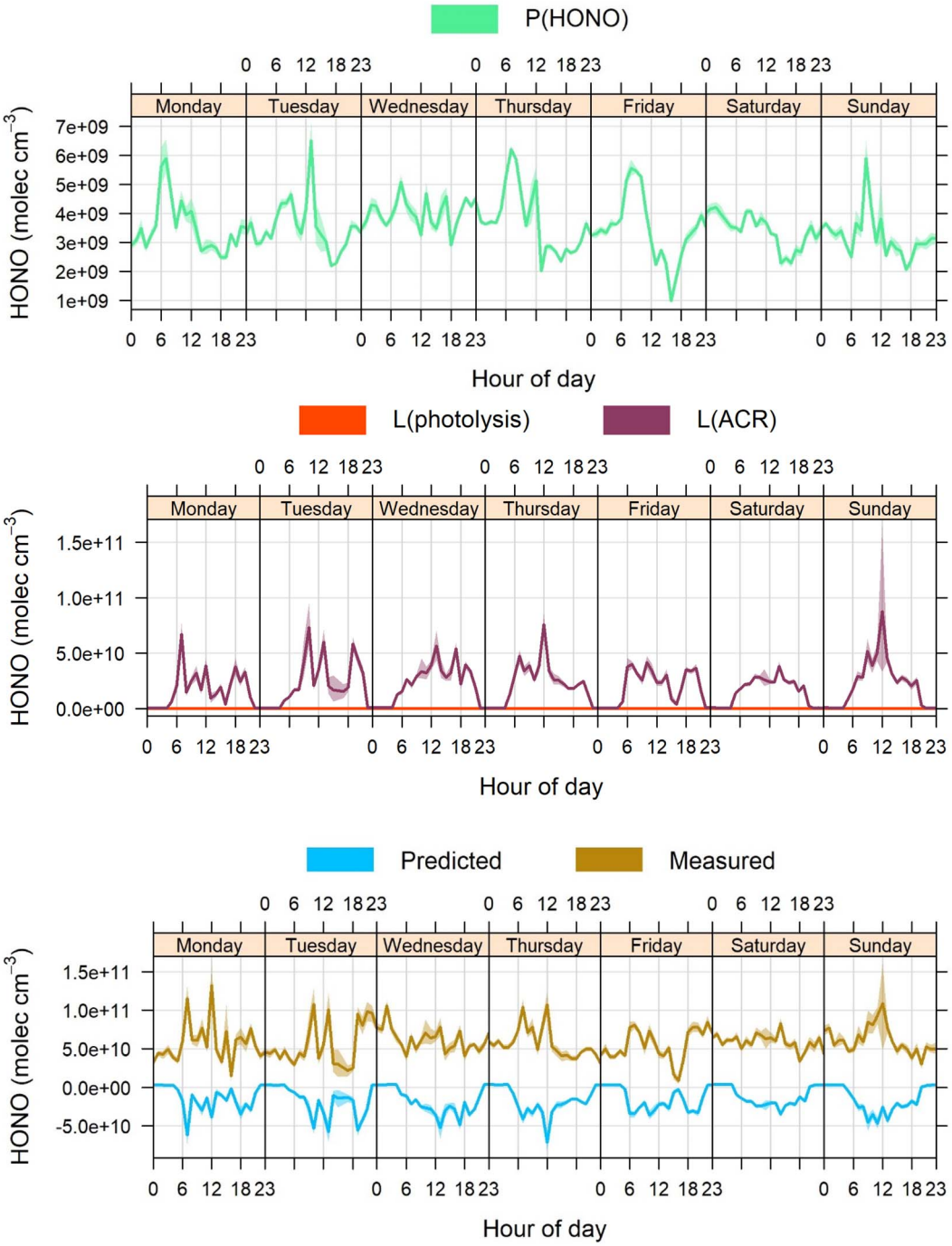

Fig. 6 Mean diurnal predicted HONO levels calculated from production by NO_2 uptake on surfaces (top) and loss by photolysis and ventilation (middle) compared to measured HONO by day of week (bottom), using a γ_{NO_2} of 2×10^{-6} and a nighttime ACR of 0.5 h^{-1}. The shaded areas represent the 95% confidence interval of the mean. Ventilation dominates the fate of HONO leading to predicted concentrations lower than measured, implicating the presence of additional sources.

observed higher NO_2 reactivity. Overall, residential and commercial kitchen space controls over HONO mixing ratios are similar in mechanism but occurring at a larger magnitude in this commercial space with a potential legacy of less well-ventilated operation conditions to facilitate large persistent pollutant reservoirs. The limited information on air infiltration rates in commercial buildings, as well as the uncertainty in the conversion of NO_2 on the heavily impacted kitchen surfaces, can lead to outcomes that are somewhat different from those depicted from our best estimates discussed here (Table S2†). Given the strong departure from prior reports in our observed NO_2 loss rates, the NO_2-dominant scenario is an upper limit

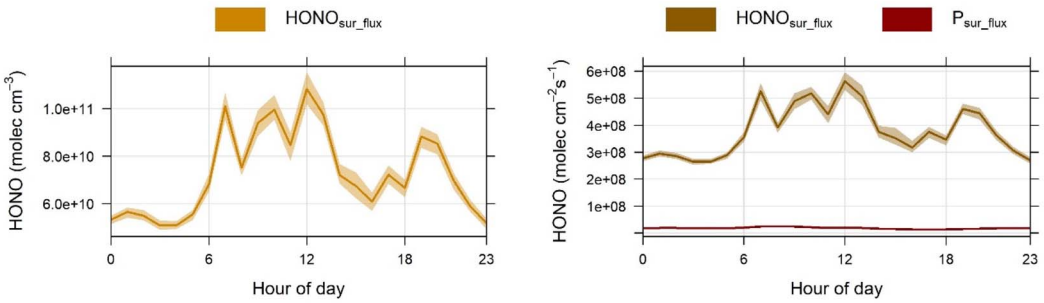

Fig. 7 (Left) Mean diurnal trends of HONO levels originating from surface emissions ($HONO_{sur\_flux}$) using E7, and (Right) the calculated fluxes required to maintain these levels from surface emissions ($HONO_{sur\_flux}$) and NO_2 uptake (P_{sur_flux}). The shaded areas represent the 95% confidence interval of the mean. Note the different *y*-axis scales and units.

without precedent and should be treated as such in terms of its explanatory power. This is the only model scenario where the nighttime HONO levels can be reasonably captured by NO_2 heterogeneous reactions. Regardless, our more modest model runs and this upper limit all agree on the presence of a substantial and sustained HONO surface source to reconcile the observations when this kitchen space is actively ventilated.

3.3.5 Surface reservoirs of other N_r species. In addition to HONO, the tN_r measurements indicate that neutral and basic N_r species also had stable background levels, when direct emissions were absent (Fig. 2). The average daytime and night-time levels of the neutral fraction were 2.9 ± 1.4 and 3.0 ± 0.22 ppbv, while they were 7.4 ± 0.7 and 5.8 ± 0.4 ppbv for the basic N_r fraction. Similarly, when comparing PTR-MS ion signals pre- and post-ventilation start-up (*i.e.*, 3–4 am *vs.* 6–7 am), we observed 90% of ions with signal differences that were statistically insignificant.[40] Specifically, notable ions that exhibit these trends include acetonitrile, triethylamine, monochloramine and most other N-containing species (Fig. S15†).

The similar levels between day and night for the majority of N_r ions, despite the difference in ACR, also point to a very fast and strong source to compete with the very high ACR in the kitchen. Otherwise, signal increases would have been observed overnight, when there were no cooking emissions present, and these would have dropped dramatically upon ventilation power up in the morning. Taken together, these observations suggest a significant surface reservoir for these species also with rapid equilibrium control on indoor air composition. These observations also appear to reflect the decades-long legacy of surface contamination built up in the ventilation system and kitchen, such as from use of cooking oils.[84] Similar findings have been reported for the persistence of SVOCs in the indoor air of an office,[85] and the accumulation of gases like HONO in a test house.[49] Surface fluxes for a subset of VOCs measured by the PTR-MS are shown in Table S3.† Fluxes were estimated by focusing on measured air concentrations from 6–7 am, while ventilation in the kitchen was powered on but no other sources except surfaces existed in the kitchen and no changes to VOC signals were observed. This calculation assumes constant VOC surface flux rate throughout the ventilated period in the kitchen (6 am to 10 pm) and represents the net effect of surface emissions and deposition.

Compared to past floor area specific VOC emission factors from a newly constructed residential test facility with low VOC-emitting materials, and comparisons to other occupied or unoccupied homes therein,[86] surface fluxes from this commercial kitchen generally fell within similar orders of magnitude but are compound-dependent. For example, ethanol fluxes were about 6 times higher in the kitchen than in Poppendieck *et al.*,[86] which is consistent with cooking activity in the kitchen being a major source. Acetone, acetic acid, toluene, and terpene fluxes were similar in the commercial kitchen and residential environments. Hexanal fluxes in the kitchen were about 1 order of magnitude lower than the homes, while D5-siloxane fluxes were 2 orders of magnitude greater in the kitchen which is consistent with its high occupancy with sometimes more than ten staff, relative to when unoccupied.

Surface fluxes of nitrogen containing species have been observed indoors in other work, albeit they seldom have a decades-long legacy of intense use for 10 hours per day.[87] For example, Wang *et al.*[20] studied indoor surfaces as dynamic temporary reservoirs for volatile species at the HOMEChem test house and observed that ammonia participated in rapid gas–surface exchange, with a response time to return to steady state mixing ratios after enhanced ventilation periods ranging from 500–2500 s. This response time was longer than that for many of the other VOCs studied, suggesting that NH_3 could perhaps be more strongly sorbed to surfaces. Similar observations were also made by Wang *et al.*[32] for isocyanic acid (HNCO) during the same field campaign, with mixing ratios increasing as a function of temperature, with increased evaporation from surfaces occurring at higher air and surface temperatures. Surface reservoirs of acetonitrile indoors were observed by Arata *et al.*[88] who reported stable levels of <1 ppb yet calculated a net loss of 0.09 mg h^{-1} indoors during the HOMEChem campaign based on the indoor to outdoor ratio decreasing over the day. In contrast, the majority of the other VOCs reported by Arata *et al.*[88] exhibited a net gain indoors.

3.3.6 Implications of significant surface reservoirs. The results from the current work point to indoor surfaces acting as significant reservoirs and therefore sources for a range of acidic, neutral and basic N_r species. As demonstrated for HONO, the magnitude of this source can be as significant as other primary sources (*e.g.* combustion) and therefore warrants further work

to better understand the role surfaces play in controlling indoor levels of such gases.[89] This is especially pressing for indoor areas with large emission sources (*e.g.* kitchens) that operate intensively and could do so for decades without substantial changes in operation conditions, that may lead to extremely deep reservoirs of such species such that they come to dominate over other primary sources when changes to address direct emissions are implemented. Indoor pollutants can also be ventilated outdoors, and as such, the chemical and physical properties governing the fluxes from surfaces indoors may not only just affect the indoor air, but outdoor air quality and warrants further study. As many of these reported findings were unexpected, it remains unclear how prevalent such indoor reservoirs as the one studied here are and if it would be possible to deplete them without complete removal of the materials comprising the kitchen surfaces and HVAC ducting.

4. Conclusions

High time resolution measurements of the first gas phase tN_r budget in a commercial kitchen identified the contributions of a variety of key N_r species and determined the extent that this budget can be closed with modern high time resolution analytical instrumentation. The mean diurnal tN_r budget was not closed using the measured levels of NO, NO_2, HONO and basic N_r (*e.g.* NH_3 and amines); a substantial missing fraction (*ca.* 5 ppbv) was found. Using supporting PTR-MS measurements of calibrated N-containing species, the missing fraction of N_r was found to be partially closed by the neutral organic species acetonitrile, propionamide, pyrrole and acrylonitrile, but with roughly 3 ppbv of the missing fraction remaining unaccounted for and composed of a wide variety of chemical structures that were not calibrated on the PTR-MS. That these neutral species could not fully account for the observed missing fraction may point to there being notable contributions from unheralded N-containing species indoors.

Cooking events in the kitchen produced a diverse and numerous array of N-containing species detected by the PTR-MS. This variety was due to the complexity of cooking occurring in the kitchen with different cooking areas, combinations of different ingredients and appliances, as well as overlapping meal preparations and techniques. This made identifying specific tracers for cooking a particular dish or single form of food challenging. When grouped by their broad molecular formulae, oxygenated N-containing class ions ($C_{1-12}H_{3-24}O_{1-4}N_{1-3}$), consistent with the known formulae of amides or other combinations of reduced nitrogen groups with oxygenated groups, appear to be good tracers for meat cooking. This could be the focus of future targeted research under controlled lab conditions and from surveys of urban air impacted by cooking to explore if specific amides could be used as such tracers.

Many of the highest abundance N-containing ions measured by the PTR-MS were chlorinated, with monochloramine the dominant ion in this class. The observed elevated levels of monochloramine were surprising and found to be emitted from use of HOCl based cleaners in the kitchen *via* direct emissions[37] or surface reactions with reduced N-containing compounds. This is concerning due to the established toxicity of NH_2Cl, and therefore emphasizes an emerging need to understand worker exposure levels with more accurate measurements in the future. Unfortunately, quantification of NH_2Cl with PTR-MS remains challenging and will need improvement to obtain quantification *via* both the PTR-MS and tN_r instruments, as such chlorinated anthropogenic compounds are being recognized to have increasing importance for both indoor and outdoor atmospheric chemistry.[36,54] As this particular PTR-MS is not sensitive to higher order chloramines, differences in cleaning practises in a commercial kitchen compared to domestic settings (*e.g.* cleaners employed or limiting reagents with respect to surface composition) and changes in the relative emissions of these molecules remains an open line of inquiry. The discrepancy between these observations and those made prior is also related to differences in the sensitivity and selectivity of different atmospheric chemical ionisation mass spectrometers to these compounds, based on the reagent ion, and warrants further investigation and optimization.

Throughout the measurement period, levels of HONO were relatively stable day and night, despite the very large changes in ACR, pointing to gas-phase HONO being in equilibrium with a large reservoir present on the surfaces in the kitchen. We used a simple chemical model constructed with production and loss processes bounded by our observations or those from others. It was found that the predicted HONO was always lower than the measured HONO under the best estimates for NO_2 heterogeneous uptake. Overall, HONO in the commercial kitchen was found to be mostly produced from surfaces fluxes, while NO_2 reaction played a minor supporting role in controlling HONO, where only the most extreme NO_2 reactivity conditions put the two processes on parity during the day or dominated explanatory power under low ventilation conditions. A similar lack of diurnal patterns as seen for HONO were observed for the neutral and basic N_r species acetonitrile and triethylamine, as well as many other N-containing species. Thus, the stable levels despite high ACR points to large reservoirs of N_r present on the surfaces in this commercial kitchen and was a surprising finding in this study. The magnitude of the reservoir in the indoor space, by mass, and how one might conduct its amelioration warrants further research.

Data availability

The data from this study are available upon request from the authors.

Conflicts of interest

There are no conflicts to declare.

Acknowledgements

We would like to acknowledge the entire research team who contributed to this field campaign: beyond the authors listed here, we extend our thanks to C. J. Young and L. Salehpoor (York University), T. Kahan (University of Saskatchewan). We thank C. J. Young for the loan of the EC9841 and Serinus 10

during the kitchen observations. We also wish to thank the building operators, facilities managers, and kitchen staff for access to the observation space, mechanical rooms, operations and sales logs, and ventilation data. ML acknowledges support through the Harold I. Schiff award in atmospheric chemistry. JCD and AWHC acknowledge funding from the Canada Research Chairs program (CRC-2019-00028); TV, ML, LRC, JCD and JPDA acknowledge funding from the Alfred P. Sloan Foundation CIE Program (G-2019-11404, G-2018-11062, G-2018-11051), and NSERC Discovery Grants and Discovery Launch Supplement (RGPIN-2020-06166 and DGECR-2020-00186).

References

1 J. P. D. Abbatt and C. Wang, The atmospheric chemistry of indoor environments, *Environ. Sci.: Process. Impacts*, 2020, **22**, 25–48.

2 J. M. Roberts, C. E. Stockwell, R. J. Yokelson, J. de Gouw, Y. Liu, V. Selimovic, A. R. Koss, K. Sekimoto, M. M. Coggon, B. Yuan, K. J. Zarzana, S. S. Brown, C. Santin, S. H. Doerr and C. Warneke, The nitrogen budget of laboratory-simulated western US wildfires during the FIREX 2016 Fire Lab study, *Atmos. Chem. Phys.*, 2020, **20**, 8807–8826.

3 V. Bartolomei, E. Gomez Alvarez, J. Wittmer, S. Tlili, R. Strekowski, B. Temime-Roussel, E. Quivet, H. Wortham, C. Zetzsch, J. Kleffmann and S. Gligorovski, Combustion Processes as a Source of High Levels of Indoor Hydroxyl Radicals through the Photolysis of Nitrous Acid, *Environ. Sci. Technol.*, 2015, **49**, 6599–6607.

4 D. B. Collins, R. F. Hems, S. Zhou, C. Wang, E. Grignon, M. Alavy, J. A. Siegel and J. P. D. Abbatt, Evidence for Gas-Surface Equilibrium Control of Indoor Nitrous Acid, *Environ. Sci. Technol.*, 2018, **52**, 12419–12427.

5 S. Zhou, C. J. Young, T. C. VandenBoer, S. F. Kowal and T. F. Kahan, Time-Resolved Measurements of Nitric Oxide, Nitrogen Dioxide, and Nitrous Acid in an Occupied New York Home, *Environ. Sci. Technol.*, 2018, **52**, 8355–8364.

6 M. Dennekamp, S. Howarth, C. A. J. Dick, J. W. Cherrie, K. Donaldson and A. Seaton, Ultrafine particles and nitrogen oxides generated by gas and electric cooking, *Occup. Environ. Med.*, 2001, **58**, 511–516.

7 L. Kiyoung, X. Jianping, S. G. Alison, O. Halûk, P. L. Brian, J. W. Charles and D. S. John, Nitrous acid, nitrogen dioxide, and ozone concentrations in residential environments, *Environ. Health Perspect.*, 2002, **110**, 145–150.

8 N. A. Mullen, J. Li, M. L. Russell, M. Spears, B. D. Less and B. C. Singer, Results of the California Healthy Homes Indoor Air Quality Study of 2011-2013: impact of natural gas appliances on air pollutant concentrations, *Indoor Air*, 2016, **26**, 231–245.

9 E. D. Lebel, C. J. Finnegan, Z. Ouyang and R. B. Jackson, Methane and NO_x Emissions from Natural Gas Stoves, Cooktops, and Ovens in Residential Homes, *Environ. Sci. Technol.*, 2022, **56**, 2529–2539.

10 S. F. Kowal, S. R. Allen and T. F. Kahan, Wavelength-Resolved Photon Fluxes of Indoor Light Sources: Implications for HO_x Production, *Environ. Sci. Technol.*, 2017, **51**, 10423–10430.

11 B. Bottorff, C. Wang, E. Reidy, C. Rosales, D. K. Farmer, M. E. Vance, J. P. D. Abbatt and P. S. Stevens, Comparison of Simultaneous Measurements of Indoor Nitrous Acid: Implications for the Spatial Distribution of Indoor HONO Emissions, *Environ. Sci. Technol.*, 2022, **56**(19), 13573–13583.

12 B. J. Finlayson-Pitts, L. M. Wingen, A. L. Sumner, D. Syomin and K. A. Ramazan, The heterogeneous hydrolysis of NO_2 in laboratory systems and in outdoor and indoor atmospheres: an integrated mechanism, *Phys. Chem. Chem. Phys.*, 2003, **5**, 223–242.

13 S. Zhou, C. J. Young, T. C. VandenBoer and T. F. Kahan, Role of location, season, occupant activity, and chemistry in indoor ozone and nitrogen oxide mixing ratios, *Environ. Sci.: Process. Impacts*, 2019, **21**, 1374–1383.

14 C. Arata, K. J. Zarzana, P. K. Misztal, Y. Liu, S. S. Brown, W. W. Nazaroff and A. H. Goldstein, Measurement of NO_3 and N_2O_5 in a Residential Kitchen, *Environ. Sci. Technol. Lett.*, 2018, **5**, 595–599.

15 D. K. Farmer, M. E. Vance, D. Poppendieck, J. Abbatt, M. R. Alves, K. C. Dannemiller, C. Deeleepojananan, J. Ditto, B. Dougherty and O. R. Farinas, The chemical assessment of surfaces and air (CASA) study: using chemical and physical perturbations in a test house to investigate indoor processes, *Environ. Sci. Process. Impacts.*, 2024, DOI: **10.1039/D4EM00209A**.

16 M. F. Link, J. Li, J. C. Ditto, H. Huynh, J. Yu, S. M. Zimmerman, K. L. Rediger, A. Shore, J. P. D. Abbatt and L. A. Garofalo, Ventilation in a Residential Building Brings Outdoor NOx Indoors with Limited Implications for VOC Oxidation from NO_3 Radicals, *Environ. Sci. Technol.*, 2023, **57**, 16446–16455.

17 A. Moravek, T. C. Vandenboer, Z. A. Finewax, D. Pagonis, B. Nault, W. L. Brown, D. A. Day, A. V. Handshy, H. Stark, P. Ziemann, J. L. Jimenez, J. de Gouw and C. J. Young, Reactive Chlorine Emissions from Cleaning and Reactive Nitrogen Chemistry in an Indoor Athletic Facility, *Environ. Sci. Technol.*, 2022, **56**(22), 15408–15416.

18 T. C. VandenBoer, S. S. Brown, J. G. Murphy, W. C. Keene, C. J. Young, A. A. P. Pszenny, S. Kim, C. Warneke, J. A. de Gouw and J. R. Maben, Understanding the role of the ground surface in HONO vertical structure: high resolution vertical profiles during NACHTT-11, *J. Geophys. Res. Atmos.*, 2013, **118**, 10–155.

19 T. C. VandenBoer, M. Z. Markovic, J. E. Sanders, X. Ren, S. E. Pusede, E. C. Browne, R. C. Cohen, L. Zhang, J. Thomas and W. H. Brune, Evidence for a nitrous acid (HONO) reservoir at the ground surface in Bakersfield, CA, during CalNex 2010, *J. Geophys. Res. Atmos.*, 2014, **119**, 9093–9106.

20 C. Wang, D. B. Collins, C. Arata, A. H. Goldstein, J. M. Mattila, D. K. Farmer, L. Ampollini, P. F. DeCarlo, A. Novoselac, M. E. Vance, W. W. Nazaroff and J. P. D. Abbatt, Surface reservoirs dominate dynamic gas-surface partitioning of many indoor air constituents, *Sci. Adv.*, 2020, **6**, eaay8973.

21 A. Klosterköther, R. Kurtenbach, P. Wiesen and J. Kleffmann, Determination of the emission indices for NO, NO_2, HONO, HCHO, CO, and particles emitted from candles, *Indoor Air*, 2021, **31**, 116–127.
22 J. Liu, H. Deng, P. S. J. Lakey, H. Jiang, M. Mekic, X. Wang, M. Shiraiwa and S. Gligorovski, Unexpectedly High Indoor HONO Concentrations Associated with Photochemical NO_2 Transformation on Glass Windows, *Environ. Sci. Technol.*, 2020, **54**, 15680–15688.
23 C. J. Young, S. Zhou, J. A. Siegel and T. F. Kahan, Illuminating the dark side of indoor oxidants, *Environ. Sci.: Process. Impacts*, 2019, **21**, 1229–1239.
24 R. Sommariva, L. R. Crilley, S. M. Ball, R. L. Cordell, L. D. J. Hollis, W. J. Bloss and P. S. Monks, Enhanced wintertime oxidation of VOCs via sustained radical sources in the urban atmosphere, *Environ. Pollut.*, 2021, **274**, 116563.
25 T. F. Kahan, C. J. Young and S. Zhou, Indoor photochemistry, in, *Handbook of Indoor Air Quality*, ed. Y. Zhang, P. K. Hopke and C. Mandin, Springer Singapore, Singapore, 2021, pp. 1–30.
26 Y. Zhao and B. Zhao, Emissions of air pollutants from Chinese cooking: a literature review, *Build. Simul.*, 2018, **11**, 977–995.
27 K. L. Abdullahi, J. M. Delgado-Saborit and R. M. Harrison, Emissions and indoor concentrations of particulate matter and its specific chemical components from cooking: a review, *Atmos. Environ.*, 2013, **71**, 260–294.
28 J. C. Ditto, J. P. D. Abbatt and A. W. H. Chan, Gas- and Particle-Phase Amide Emissions from Cooking: Mechanisms and Air Quality Impacts, *Environ. Sci. Technol.*, 2022, **56**, 7741–7750.
29 L. Ampollini, E. F. Katz, S. Bourne, Y. Tian, A. Novoselac, A. H. Goldstein, G. Lucic, M. S. Waring and P. F. DeCarlo, Observations and Contributions of Real-Time Indoor Ammonia Concentrations during HOMEChem, *Environ. Sci. Technol.*, 2019, **53**, 8591–8598.
30 J. Zeng, Z. Yu, M. Mekic, J. Liu, S. Li, G. Loisel, W. Gao, A. Gandolfo, Z. Zhou, X. Wang, H. Herrmann, S. Gligorovski and X. Li, Evolution of Indoor Cooking Emissions Captured by Using Secondary Electrospray Ionization High-Resolution Mass Spectrometry, *Environ. Sci. Technol. Lett.*, 2020, **7**, 76–81.
31 E. Reyes-Villegas, T. Bannan, M. Le Breton, A. Mehra, M. Priestley, C. Percival, H. Coe and J. D. Allan, Online Chemical Characterization of Food-Cooking Organic Aerosols: Implications for Source Apportionment, *Environ. Sci. Technol.*, 2018, **52**, 5308–5318.
32 C. Wang, J. M. Mattila, D. K. Farmer, C. Arata, A. H. Goldstein and J. P. D. Abbatt, Behavior of Isocyanic Acid and Other Nitrogen-Containing Volatile Organic Compounds in The Indoor Environment, *Environ. Sci. Technol.*, 2022, **56**, 7598–7607.
33 R. F. Hems, C. Wang, D. B. Collins, S. Zhou, N. Borduas-Dedekind, J. A. Siegel and J. P. D. Abbatt, Sources of isocyanic acid (HNCO) indoors: a focus on cigarette smoke, *Environ. Sci.: Process. Impacts*, 2019, **21**, 1334–1341.
34 J. M. Mattila, P. S. J. Lakey, M. Shiraiwa, C. Wang, J. P. D. Abbatt, C. Arata, A. H. Goldstein, L. Ampollini, E. F. Katz, P. F. DeCarlo, S. Zhou, T. F. Kahan, F. J. Cardoso-Saldaña, L. H. Ruiz, A. Abeleira, E. K. Boedicker, M. E. Vance and D. K. Farmer, Multiphase Chemistry Controls Inorganic Chlorinated and Nitrogenated Compounds in Indoor Air during Bleach Cleaning, *Environ. Sci. Technol.*, 2020, **54**, 1730–1739.
35 Z. Finewax, D. Pagonis, M. S. Claflin, A. V Handschy, W. L. Brown, O. Jenks, B. A. Nault, D. A. Day, B. M. Lerner, J. L. Jimenez, P. J. Ziemann and J. A. de Gouw, Quantification and source characterization of volatile organic compounds from exercising and application of chlorine-based cleaning products in a university athletic center, *Indoor Air*, 2021, **31**, 1323–1339.
36 A. A. Angelucci, L. R. Crilley, R. Richardson, T. S. E. Valkenburg, P. S. Monks, J. M. Roberts, R. Sommariva and T. C. VandenBoer, Elevated levels of chloramines and chlorine detected near an indoor sports complex, *Environ. Sci.: Process. Impacts*, 2023, **25**, 304–313.
37 J. P. S. Wong, N. Carslaw, R. Zhao, S. Zhou and J. P. D. Abbatt, Observations and impacts of bleach washing on indoor chlorine chemistry, *Indoor Air*, 2017, **27**, 1082–1090.
38 S. Kim, J. Machesky, D. R. Gentner and A. A. Presto, Real-world observations of reduced nitrogen and ultrafine particles in commercial cooking organic aerosol emissions, *Atmos. Chem. Phys.*, 2024, **24**, 1281–1298.
39 T. J. Carter, D. R. Shaw, D. C. Carslaw and N. Carslaw, Indoor cooking and cleaning as a source of outdoor air pollution in urban environments, *Environ. Sci.: Process. Impacts*, 2024, **26**, 975–990.
40 J. C. Ditto, L. R. Crilley, M. Lao, T. C. VandenBoer, J. P. D. Abbatt and A. W. H. Chan, Indoor and outdoor air quality impacts of cooking and cleaning emissions from a commercial kitchen, *Environ. Sci.: Process. Impacts*, 2023, **25**, 964–979.
41 L. R. Crilley, M. Lao, L. Salehpoor and T. C. VandenBoer, Emerging investigator series: an instrument to measure and speciate the total reactive nitrogen budget indoors: description and field measurements, *Environ. Sci.: Process. Impacts*, 2023, **25**, 389–404.
42 D. C. Carslaw and K. Ropkins, openair — an R package for air quality data analysis, *Environ. Model. Softw.*, 2012, **27–28**, 52–61.
43 M. Mendez, N. Blond, D. Amedro, D. A. Hauglustaine, P. Blondeau, C. Afif, C. Fittschen and C. Schoemaecker, Assessment of indoor HONO formation mechanisms based on in situ measurements and modeling, *Indoor Air*, 2017, **27**, 443–451.
44 T. C. VandenBoer, C. J. Young, R. K. Talukdar, M. Z. Markovic, S. S. Brown, J. M. Roberts and J. G. Murphy, Nocturnal loss and daytime source of nitrous acid through reactive uptake and displacement, *Nat. Geosci.*, 2015, **8**, 55–60.
45 M. E. Monge, B. D'Anna and C. George, Nitrogen dioxide removal and nitrous acid formation on titanium oxide

surfaces-an air quality remediation process?, *Phys. Chem. Chem. Phys.*, 2010, **12**, 8991–8998.
46 R. Ammar, M. E. Monge, C. George and B. D'Anna, Photoenhanced NO_2 Loss on Simulated Urban Grime, *ChemPhysChem*, 2010, **11**, 3956–3961.
47 M. Brauer, P. B. Ryan, H. H. Suh, P. Koutrakis, J. D. Spengler, N. P. Leslie and I. H. Billick, Measurements of nitrous acid inside two research houses, *Environ. Sci. Technol.*, 1990, **24**, 1521–1527.
48 F. Vichi, L. Mašková, M. Frattoni, A. Imperiali and J. Smolík, Simultaneous measurement of nitrous acid, nitric acid, and nitrogen dioxide by means of a novel multipollutant diffusive sampler in libraries and archives, *Herit. Sci.*, 2016, **4**, 4.
49 C. Wang, B. Bottorff, E. Reidy, C. M. F. Rosales, D. B. Collins, A. Novoselac, D. K. Farmer, M. E. Vance, P. S. Stevens and J. P. D. Abbatt, Cooking, Bleach Cleaning, and Air Conditioning Strongly Impact Levels of HONO in a House, *Environ. Sci. Technol.*, 2020, **54**, 13488–13497.
50 S. Robbana-Barnat, M. Rabache, E. Rialland and J. Fradin, Heterocyclic amines: occurrence and prevention in cooked food, *Environ. Health Perspect.*, 1996, **104**, 280–288.
51 K. Kikugawa, Formation of mutagens, 2-amino-3, 8-dimethylimidazo [4, 5-# f] quinoxaline (MeIQx) and 2-amino-3, 4, 8-trimethylimidazo [4, 5-# f] quinoxaline (4, 8-DiMeIQx), in heated fish meats, *Mutat. Res. Mol. Mech. Mutagen.*, 1987, **179**, 5–14.
52 L. Salehpoor and T. C. VandenBoer, Suppressor and calibration standard limitations in cation chromatography of ammonium and 10 alkylamines in atmospheric samples, *Anal. Methods*, 2023, **15**, 3822–3842.
53 K. Sekimoto, S.-M. Li, B. Yuan, A. Koss, M. Coggon, C. Warneke and J. de Gouw, Calculation of the sensitivity of proton-transfer-reaction mass spectrometry (PTR-MS) for organic trace gases using molecular properties, *Int. J. Mass Spectrom.*, 2017, **421**, 71–94.
54 C. Wang, J. Liggio, J. J. B. Wentzell, S. Jorga, A. Folkerson and J. P. D. Abbatt, Chloramines as an important photochemical source of chlorine atoms in the urban atmosphere, *Proc. Natl. Acad. Sci. U. S. A.*, 2023, **120**, e2220889120.
55 T. Wu, T. Földes, L. T. Lee, D. N. Wagner, J. Jiang, A. Tasoglou, B. E. Boor and E. R. I. I. I. Blatchley, Real-Time Measurements of Gas-Phase Trichloramine (NCl3) in an Indoor Aquatic Center, *Environ. Sci. Technol.*, 2021, **55**, 8097–8107.
56 T. C. Furlani, R. Ye, J. Stewart, L. R. Crilley, P. M. Edwards, T. F. Kahan and C. J. Young, Development and validation of a new in situ technique to measure total gaseous chlorine in air, *Atmos. Meas. Tech.*, 2023, **16**, 181–193.
57 M. A. Bari, W. B. Kindzierski, A. J. Wheeler, M.-È. Héroux and L. A. Wallace, Source apportionment of indoor and outdoor volatile organic compounds at homes in Edmonton, Canada, *Build. Environ.*, 2015, **90**, 114–124.
58 R. Sheu, C. Stönner, J. C. Ditto, T. Klüpfel, J. Williams and D. R. Gentner, Human transport of thirdhand tobacco smoke: a prominent source of hazardous air pollutants into indoor nonsmoking environments, *Sci. Adv.*, 2022, **6**, eaay4109.
59 A. Arı, P. Ertürk Arı, S. Yenisoy-Karakaş and E. O. Gaga, Source characterization and risk assessment of occupational exposure to volatile organic compounds (VOCs) in a barbecue restaurant, *Build. Environ.*, 2020, **174**, 106791.
60 X. Wang, Y. Wang, G. Hu, D. Hong, T. Guo, J. Li, Z. Li and M. Qiu, Review on factors affecting coffee volatiles: from seed to cup, *J. Sci. Food Agric.*, 2022, **102**, 1341–1352.
61 Y. Liu, P. K. Misztal, J. Xiong, Y. Tian, C. Arata, R. J. Weber, W. W. Nazaroff and A. H. Goldstein, Characterizing sources and emissions of volatile organic compounds in a northern California residence using space- and time-resolved measurements, *Indoor Air*, 2019, **29**, 630–644.
62 C. E. Stockwell, P. R. Veres, J. Williams and R. J. Yokelson, Characterization of biomass burning emissions from cooking fires, peat, crop residue, and other fuels with high-resolution proton-transfer-reaction time-of-flight mass spectrometry, *Atmos. Chem. Phys.*, 2015, **15**, 845–865.
63 S. A. O. Adeyeye, Heterocyclic Amines and Polycyclic Aromatic Hydrocarbons in Cooked Meat Products: A Review, *Polycycl. Aromat. Compd.*, 2020, **40**, 1557–1567.
64 L. Hashim and H. Chaveron, Use of methylpyrazine ratios to monitor the coffee roasting, *Food Res. Int.*, 1995, **28**, 619–623.
65 E. C. Coleman and C.-T. Ho, Chemistry of baked potato flavor. 1. Pyrazines and thiazoles identified in the volatile flavor of baked potato, *J. Agric. Food Chem.*, 1980, **28**, 66–68.
66 I. M. Weiss, C. Muth, R. Drumm and H. O. K. Kirchner, Thermal decomposition of the amino acids glycine, cysteine, aspartic acid, asparagine, glutamic acid, glutamine, arginine and histidine, *BMC Biophys.*, 2018, **11**, 2.
67 E. G. Vilar, M. G. O'Sullivan, J. P. Kerry and K. N. Kilcawley, Volatile organic compounds in beef and pork by gas chromatography-mass spectrometry: a review, *Sep. Sci.*, 2022, **5**, 482–512.
68 M. M. Coggon, C. E. Stockwell, L. Xu, J. Peischl, J. B. Gilman, A. Lamplugh, H. J. Bowman, K. Aikin, C. Harkins and Q. Zhu, Contribution of cooking emissions to the urban volatile organic compounds in Las Vegas, NV, *Atmos. Chem. Phys.*, 2024, **24**, 4289–4304.
69 F. Klein, S. M. Platt, N. J. Farren, A. Detournay, E. A. Bruns, C. Bozzetti, K. R. Daellenbach, D. Kilic, N. K. Kumar, S. M. Pieber, J. G. Slowik, B. Temime-Roussel, N. Marchand, J. F. Hamilton, U. Baltensperger, A. S. H. Prévôt and I. El Haddad, Characterization of Gas-Phase Organics Using Proton Transfer Reaction Time-of-Flight Mass Spectrometry: Cooking Emissions, *Environ. Sci. Technol.*, 2016, **50**, 1243–1250.
70 J. J. Schauer, M. J. Kleeman, G. R. Cass and B. R. T. Simoneit, Measurement of Emissions from Air Pollution Sources. 4. C1−C27 Organic Compounds from Cooking with Seed Oils, *Environ. Sci. Technol.*, 2002, **36**, 567–575.
71 W. W. Nazaroff, Residential air-change rates: a critical review, *Indoor Air*, 2021, **31**, 282–313.
72 A. Gandolfo, L. Rouyer, H. Wortham and S. Gligorovski, The influence of wall temperature on NO_2 removal and HONO

levels released by indoor photocatalytic paints, *Appl. Catal., B*, 2017, **209**, 429–436.

73 E. G. Alvarez, M. Sörgel, S. Gligorovski, S. Bassil, V. Bartolomei, B. Coulomb, C. Zetzsch and H. Wortham, Light-induced nitrous acid (HONO) production from NO_2 heterogeneous reactions on household chemicals, *Atmos. Environ.*, 2014, **95**, 391–399.

74 T. Wainman, C. J. Weschler, P. J. Lioy and J. Zhang, Effects of surface type and relative humidity on the production and concentration of nitrous acid in a model indoor environment, *Environ. Sci. Technol.*, 2001, **35**, 2200–2206.

75 R. Kurtenbach, K. H. Becker, J. A. G. Gomes, J. Kleffmann, J. C. Lörzer, M. Spittler, P. Wiesen, R. Ackermann, A. Geyer and U. Platt, Investigations of emissions and heterogeneous formation of HONO in a road traffic tunnel, *Atmos. Environ.*, 2001, **35**, 3385–3394.

76 M. R. Canagaratna, J. L. Jimenez, J. H. Kroll, Q. Chen, S. H. Kessler, P. Massoli, L. Hildebrandt Ruiz, E. Fortner, L. R. Williams, K. R. Wilson, J. D. Surratt, N. M. Donahue, J. T. Jayne and D. R. Worsnop, Elemental ratio measurements of organic compounds using aerosol mass spectrometry: characterization, improved calibration, and implications, *Atmos. Chem. Phys.*, 2015, **15**, 253–272.

77 L. J. Kramer, L. R. Crilley, T. J. Adams, S. M. Ball, F. D. Pope and W. J. Bloss, Nitrous acid (HONO) emissions under real-world driving conditions from vehicles in a UK road tunnel, *Atmos. Chem. Phys.*, 2020, **20**, 5231–5248.

78 Y. Liu, K. Lu, Y. Ma, X. Yang, W. Zhang, Y. Wu, J. Peng, S. Shuai, M. Hu and Y. Zhang, Direct emission of nitrous acid (HONO) from gasoline cars in China determined by vehicle chassis dynamometer experiments, *Atmos. Environ.*, 2017, **169**, 89–96.

79 F. Spataro and A. Ianniello, Sources of atmospheric nitrous acid: state of the science, current research needs, and future prospects, *J. Air Waste Manage. Assoc.*, 2014, **64**, 1232–1250.

80 R. Bröske, J. Kleffmann and P. Wiesen, Heterogeneous conversion of NO_2 on secondary organic aerosol surfaces: a possible source of nitrous acid (HONO) in the atmosphere?, *Atmos. Chem. Phys.*, 2003, **3**, 469–474.

81 J. Kleffmann, K. H. Becker and P. Wiesen, Heterogeneous NO_2 conversion processes on acid surfaces: possible atmospheric implications, *Atmos. Environ.*, 1998, **32**, 2721–2729.

82 M. A. Donaldson, A. E. Berke and J. D. Raff, Uptake of Gas Phase Nitrous Acid onto Boundary Layer Soil Surfaces, *Environ. Sci. Technol.*, 2014, **48**, 375–383.

83 M. A. Donaldson, D. L. Bish and J. D. Raff, Soil surface acidity plays a determining role in the atmospheric-terrestrial exchange of nitrous acid, *Proc. Natl. Acad. Sci. U. S. A.*, 2014, **111**, 18472–18477.

84 Z. Zhou, L. R. Crilley, J. C. Ditto, T. C. VandenBoer and J. P. D. Abbatt, Chemical Fate of Oils on Indoor Surfaces: Ozonolysis and Peroxidation, *Environ. Sci. Technol.*, 2023, **57**, 15546–15557.

85 Y. Li, L. He, D. Xie, A. Zhao, L. Wang, N. M. Kreisberg, J. Jayne and Y. Liu, Strong temperature influence and indiscernible ventilation effect on dynamics of some semivolatile organic compounds in the indoor air of an office, *Environ. Int.*, 2022, **165**, 107305.

86 D. G. Poppendieck, L. C. Ng, A. K. Persily and A. T. Hodgson, Long term air quality monitoring in a net-zero energy residence designed with low emitting interior products, *Build. Environ.*, 2015, **94**, 33–42.

87 J. C. Ditto, M. Webb, H. N. Huynh, J. Yu, G. C. Morrison, B. J. Turpin, M. R. Alves, K. Mayer, M. F. Link, A. H. Goldstein, D. Poppendieck, M. E. Vance, D. K. Farmer, A. W. H. Chan and J. P. D. Abbatt, The Role of Indoor Surface pH in Controlling the Fate of Acids and Bases in an Unoccupied Residence, *ACS ES&T Air*, 2024, **1**(9), 1015–1027, DOI: **10.1021/acsestair.4c00044**.

88 C. Arata, P. K. Misztal, Y. Tian, D. M. Lunderberg, K. Kristensen, A. Novoselac, M. E. Vance, D. K. Farmer, W. W. Nazaroff and A. H. Goldstein, Volatile organic compound emissions during HOMEChem, *Indoor Air*, 2021, **31**, 2099–2117.

89 W. D. Fahy, F. Wania and J. P. D. Abbatt, When Does Multiphase Chemistry Influence Indoor Chemical Fate?, *Environ. Sci. Technol.*, 2024, **58**, 4257–4267.

